3 INTRODUCTION TO THE GEOPHYSICAL METHODS APPLICABLE TO COAL

Stoffel Fourie, Michael van Schoor, Declan Vogt, Jan van der Walt, Agnes Jikelo, Geoff Campbell, Alten du Plessis

CHAPTER OUTLINE

▶ Magnetic method

▶ Gravity method

▶ Electrical methods (resistivity and induced polarisation)

▶ Ground-penetrating radar (GPR)

▶ Frequency-domain electromagnetic method

▶ Time-domain or transient electromagnetic methods (TDEM or TEM)

▶ Controlled-source audiomagnetotelluric method (CSAMT)

▶ Seismic refraction

▶ Seismic reflection

▶ Multichannel analysis of surface waves (MASW)

▶ Wireline logging

This chapter introduces a range of geophysical methods that may be applicable to coal mining and exploration problems. The focus of these discussions is on emphasising the link between geology and physics – and how the different geophysical methods exploit physics to infer geology.

▶ Magnetic method

Many geological structures and formations behave like large buried magnets due to their magnetic constituents. The result is that these structures and formations are associated with a localised magnetic field, which is superimposed on the Earth's normal magnetic field. If measurements of the magnetic field are taken in the vicinity of such structures or formations, it will show variations (anomalies) from the undisturbed magnetic field of the Earth. These anomalies can be small or large, and may either add to or subtract from the Earth's local magnetic field. The size and shape

Figure 3.1 Magnetic minerals: magnetite (Fe_3O_4), pyrrhotite (FeS) and ilmenite ($FeTiO_3$) *(Photos sourced from* www.irocks.com *and used with permission.)*

of the anomalies depend on the geometry and depth of the anomalous structure, the degree of magnetisation and the direction of the magnetisation with respect to the Earth's magnetic field. Magnetic surveys aim to derive these subsurface parameters from the observed magnetic anomalies.

Magnetic minerals such as magnetite, pyrrhotite and ilmenite are widely distributed throughout the Earth's crust (**Figure 3.1**). Magnetite concentration is the single most important factor in the magnetic response of rocks.

Fundamental principles

Earth's magnetic field

The Earth's magnetic field, which is caused by the circulation of the liquid part of the iron-rich core, resembles the field of a large bar magnet, located inside the Earth. The magnet's length appears to be about one-third of the diameter of the Earth, and it is slightly deviated from the Earth's spin axis (**Figure 3.2**). The most important effect of the Earth's magnetic field is to shield the Earth from high-energy, radioactive particles that come from the Sun. The direction of the magnetic field, with respect to the Earth's surface, is vertical at the North and South magnetic poles and horizontal at the equator. Between these two extremes the field direction is at an angle (< 90°) to the Earth's surface. The field strength is conventionally taken as positive towards the North Pole. The intensity of the Earth's magnetic field varies across the globe; it is strongest at the magnetic poles and weakest at the magnetic equator (**Figure 3.2**). The angle by which a compass deviates from true North is known as the magnetic declination at that point.

**Figure 3.2** Schematic of the Earth's magnetic field[23]
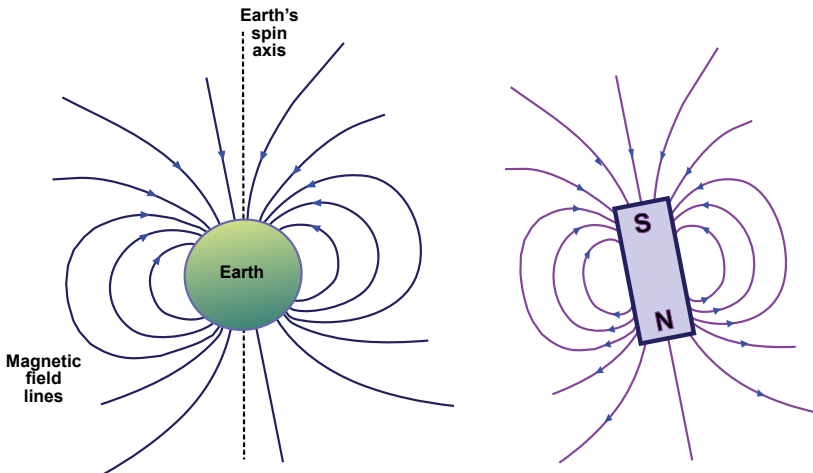
The Earth's magnetic field approximates that of a bar magnet, and magnetic North is displaced from true North (declination). The South pole of the magnet is closest to the geographic North Pole.

At any arbitrary location the Earth's magnetic field vector can be described in terms of the following components (**Figure 3.3**)[24]:

    F   Magnetic field vector

    H   Horizontal component (with Cartesian projections **X** and **Y**)

    Z   Vertical component

    I   Inclination (angle between **F** and **H**)

    D   Declination (angle between **H** and North or **X**)

Figure 3.3 Components of the Earth's magnetic field vector
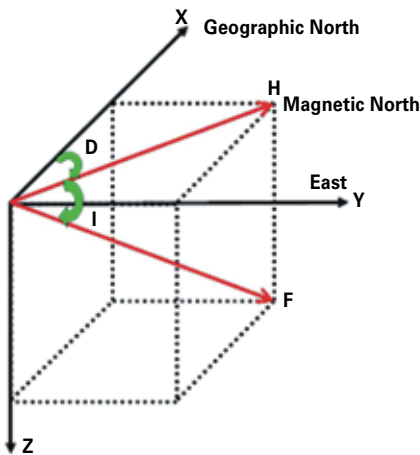
The Earth's magnetic field inclination in South Africa is approximately -60° (pointing upward), while the declination is approximately -20° (West). The magnitude of the field intensity is approximately 30 000 nT.

The Earth's magnetic field strength varies with time. The short-term variations are called diurnal variations. Significant variations occur, with periods that vary from seconds to days. These variations are not predictable and are due to the direct and indirect influence of magnetic storms created by solar winds. Diurnal variations are important in magnetic surveys, and cannot be corrected for unless they are measured. Plots of variations in the Earth's field can be obtained from the website of the International Real-time Magnetic Observatory Network (INTERMAGNET)[25]. Such data is useful for identifying periods of intense magnetic storm activity, which may adversely affect magnetic prospecting efforts. Secular variations occur slowly over periods ranging from years to thousands of years, and include polar reversals. Secular variations are, however, not important during a magnetic survey.

Induced and remanent magnetism

Magnetic anomalies in the measured Earth's magnetic field are caused by two types of magnetism: induced and remanent (permanent) magnetism. The induced magnetism of a body is in the same direction as the Earth's field, whereas remanent magnetism need not be in the same direction as the Earth's field and may even oppose it. If the Earth's present-day magnetic field could be removed, induced magnetism would disappear, but the remanent magnetism would remain.

The magnitude of induced magnetisation (*M*) is proportional to the Earth's field (*F*) and the proportionality constant is referred to as the magnetic susceptibility (*K*):

$$M = KF \hspace{2cm} \text{(3-1)}$$

As explained in Chapter 2, it is the differences in the magnetic susceptibility of rocks that are exploited by the magnetic method.

Units and terminology

The internationally accepted unit for the magnetic field strength or intensity is the Tesla (named after Nikola Tesla, the famous Serbian-American engineer and inventor). The Tesla is too large a unit for practical purposes and the nanotesla (nT, one billionth of a Tesla) is used in geophysical magnetic exploration. The name gamma (γ) was previously used instead of nanotesla.

$$1 \text{ gamma} = 1 \text{ nanotesla} = 1/1\,000\,000\,000 \text{ Tesla} = 10^{-9} \text{ Tesla.}$$

During magnetic exploration we may record anomalies (changes superimposed on the Earth's field) ranging from tens of nanoteslas to several thousand nanoteslas. The latter can be caused by large massive magnetic bodies, such as sulphides. It follows from the relationship given in **equation 3-1** that susceptibility is a dimensionless ratio that typically has values << 1 for most geological materials.

Survey strategies

Magnetic surveys may be ground-based or airborne. The purpose of the survey, the target depth, the desired resolution or mapping accuracy and the area to be covered will normally dictate the approach to be used. Where localised, metre-scale and relatively shallow targets are of interest and the size of the survey area is of the order of a few hectares, conventional ground surveys are adequate. In such cases, line and station spacings of a few metres are typically used. In some ground surveys a series of individual profiles may be acquired, but nowadays it is more common to cover areas of interest with a grid of closely spaced, parallel profiles, often in two perpendicular directions. The motivation behind this approach is twofold. Firstly, in magnetic surveying one normally tries to traverse the strike direction of anticipated targets perpendicularly; by acquiring profiles in two perpendicular directions the chances of missing target features with a specific orientation are greatly reduced. Secondly, the grid approach allows the output to be presented as contour maps, which are easier to interpret in conjunction with geological maps, etc.

Where larger and deeper targets are of interest, and information is required on a more regional scale, the airborne approach is appropriate. In airborne surveys, line spacings of 50–100 m, or even several hundred metres, may be used. As in many ground surveys, a grid of profiles is typically acquired in a weaving, criss-cross pattern.

For both ground and airborne magnetic surveys it is essential to record accurate position and altitude information for the data-processing and interpretation stages, and technologies such as GPS and LIDAR are very useful here.

In most conventional magnetic surveys the magnitude of the total magnetic field is measured. After the total field data is acquired, a number of corrections are done to produce the residual magnetic values. These corrections include the diurnal correction, a correction for variations due to changes in latitude and longitude, elevation correction and correction for the regional (background) field.

Link between magnetic measurements and Earth parameters

As was mentioned previously, the physical property of interest for the magnetic method is magnetic susceptibility, which is an indication of the degree of magnetisation of a material in response to an applied magnetic field. It was also evident from the laboratory studies summarised in Chapter 2 that the magnetic properties of rocks vary over quite a wide range of values. Igneous rocks (and to a lesser extent metamorphic rocks) generally have much higher magnetic susceptibility than typical sedimentary rocks (Table 3.1). A useful consequence is that the magnetic method can detect intrusive and altered geological structures.

Table 3.1 Laboratory study results showing that igneous rocks generally have much higher magnetic susceptibilities than sedimentary rocks[24]

| ROCK TYPE	MAGNETIC SUSCEPTIBILITY RANGE ($\times 10^6$ CGS UNITS)
Dolomite	0–75
Limestone	2–280
Sandstone	0–1 665
Shale	5–1 478
Metamorphic	0–5 824
Igneous (Acidic)	3–6 527
Igneous (Basic)	44–9 711

Magnetic survey data sets are typically presented either as one-dimensional profiles or, if an area has been traversed by a series of profiles, as two-dimensional magnetic maps. An example of a total field magnetic profile recorded over a buried dyke is shown in Figure 3.4.

The shape and magnitude of magnetic anomalies are determined by a number of factors, including the geometry of the target, target depth, target orientation (with respect to Earth's magnetic field), the survey location (properties of Earth's field) and the target's direction of magnetisation. To illustrate this point, consider the theoretical magnetic responses over a thin vertical dyke for different values of inclination, I (Figure 3.5).

Figure 3.4 Example of a total field magnetic profile over a buried dyke
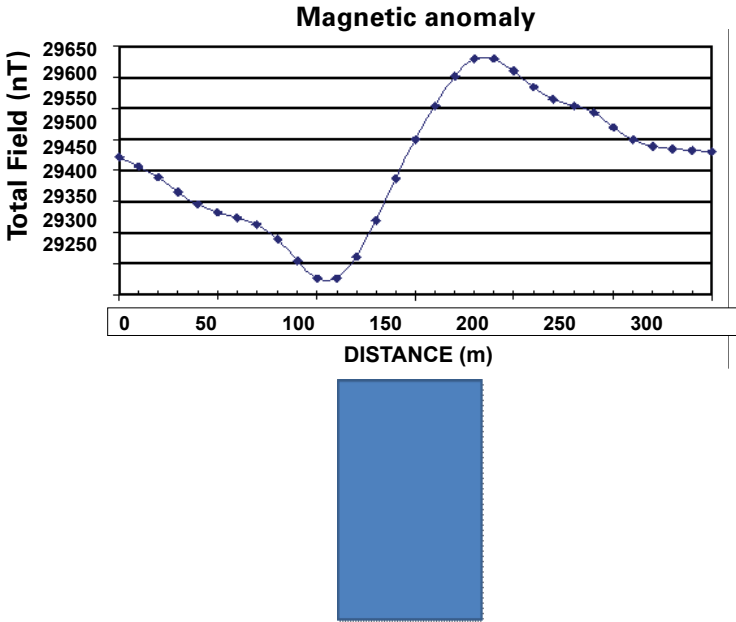
**Figure 3.5** Example of thin vertical dyke responses for different values of magnetic inclination[26]
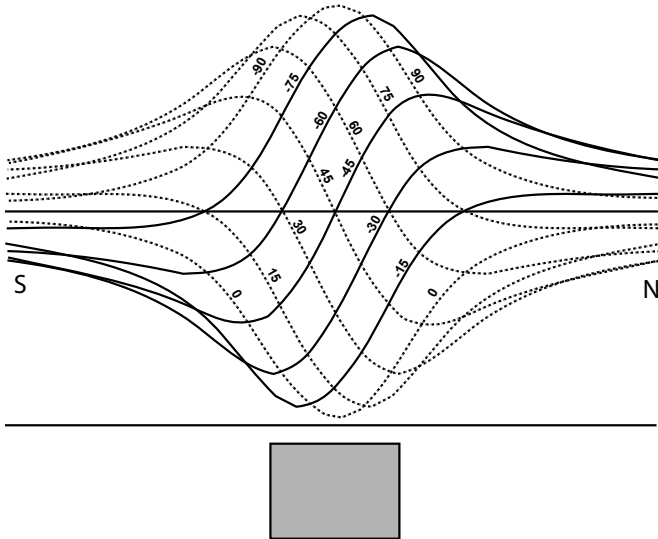
Magnetic responses over a vertical dyke as I goes from +90° to 0° (solid lines) and from 0° to -90° (dotted lines). Only induced magnetisation is considered here.

Figure 3.6 shows a typical two-dimensional magnetic contour map. The contours usually reflect the residual magnetic field; that is, the total magnetic field with the Earth's regional field removed. This is done in order to emphasise or enhance the responses from localised targets.

Interpretation of magnetic data can be as simple as qualitative 'anomaly hunting', where the user's sole aim is to locate, for example, a localised magnetic high or an anomaly associated with the edge of an intrusive body. In other cases, a more quantitative interpretation of anomalies may be required; for example, the geometry and depth of a magnetic target may be of interest. Commercially available modelling software can be used to estimate quantitative target properties through trial-and-error numerical modelling or automated inverse modelling (a computer algorithm searches for Earth models whose response matches the observed field response).

Figure 3.6 Example of a regional two-dimensional magnetic contour map[27]: high-resolution aeromagnetic image of the Witbank coalfield
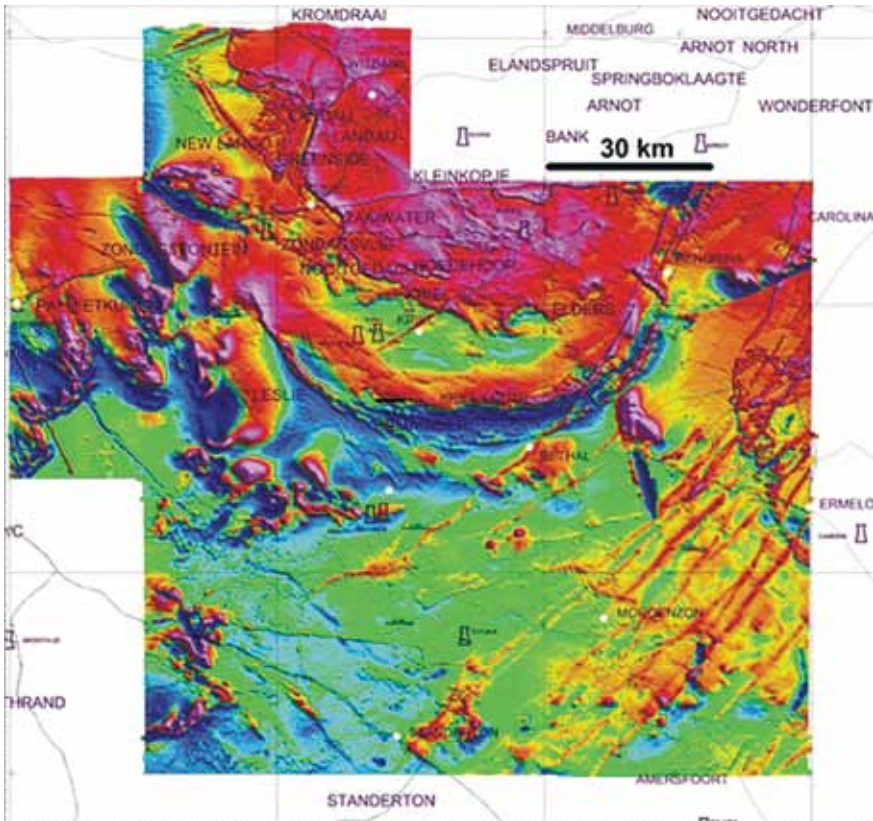
▶ Gravity method

The gravity method detects the minute changes in gravitational acceleration caused by density (mass per unit volume) variations in the Earth's crust that result from variations in mineral composition. The size and mass of geological structures and geological formations influence the behaviour of the Earth's gravity field. Thus they are associated with a localised gravity field, called the residual gravity field. This localised field is superimposed on the Earth's normal gravity field, which is called the regional gravity field. If measurements of the gravity field are taken in the vicinity of dense and massive geological structures or formations, it will show variations from the undisturbed regional gravity field. These variations, or Bouguer anomalies as they are called, can be small or large, and can either augment or diminish the Earth's regional gravity field. The size and shape of the anomalies depend on the depth of the anomalous structure and its density.

Fundamental principles

Earth's gravitational field

The Earth's gravity field and the acceleration due to gravity are controlled by two relationships[24]: Newton's universal gravity law (**Equation 3-2**) and second law of motion (**Equation 3-3**):
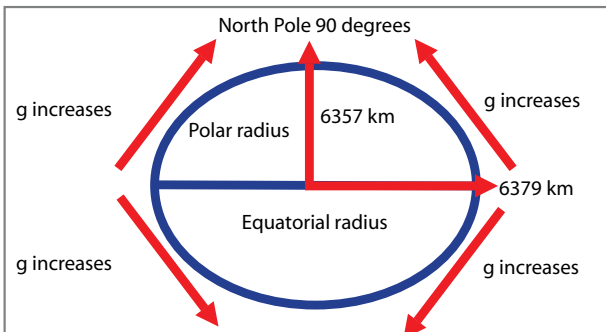
$$F = \frac{GmM_{Earth}}{R_{Earth}^2} \tag{3-2}$$

$$F = mg \tag{3-3}$$

G is the gravitational constant, M_{Earth} and m are the masses of the Earth and an arbitrary point mass at the surface of the Earth respectively, F is the force experienced due to the gravitational acceleration, R_{Earth} is the distance between the centre of the Earth and the point mass, and g is the gravitational acceleration.

The direction of the gravity field is always towards the centre of the Earth. The magnitude of the acceleration due to gravity depends on the distance from the centre of the Earth. Geodetic measurements show that the Earth is an oblate spheroid, whose radius is shorter at the Poles than at the Equator. This difference is caused by the centrifugal forces at the equator due to the rotation of the Earth around its axis[28]. The radius difference is just over 20 km, which is small compared to the Earth's mean radius of 6 370 km.

Figure 3.7 Gravity acceleration changes due to centrifugal forces, distance from the centre of the Earth and variations in latitude

North Pole 90 degrees

g increases

g increases

Polar radius

6357 km

Equatorial radius

6379 km

g increases

g increases

The main effects of the Earth's gravity field are to keep all solids and liquids closely bound to the planet, and to contribute to the heating process that drives tectonics due to pressure.

The Earth's net gravitational field strength varies with time due to the gravitational contributions of the Sun and Moon. This is referred to as the tidal variation. Significant variations (0.06 mGal) occur with periods that vary from hours to days. These variations are predictable and are compensated for during gravity surveys by the tidal correction.

Units and terminology

The internationally accepted unit for the gravitational acceleration during a gravity survey is the Gal. It is named after Galileo Galilei, the famous 16th century Italian physicist. The Gal is too large for practical purposes and the milligal (mGal) is used in geophysical exploration. A tenth of a milligal is also referred to as a gravity unit (g.u.)[28]:

1 m/s² =100 Gal. This means that 1 Gal = 1 cm/s². 1 Gal is also 1 000 mGal. The resolution of a gravity survey is 0.01 mGal, which translates into 1×10^{-5} Gal = 1×10^{-7} m/s².

During gravitational exploration we may record anomalies (changes superimposed on the Earth's field) ranging from 0.01 mGal to several tens of milligals. The latter can be caused by dense large massive bodies, such as sulphides.

Reference Geoid and the International Gravity Standardisation Network

In geodesy (study of the shape of the Earth) a *reference* geoid is a mathematically-defined surface that approximates the true geoid as closely as possible. The geoid is defined as the hypothetical (or mathematical) equipotential surface of the Earth's gravity field, and coincides closely with the undisturbed mean sea level (**Figure 3.8**). Because of their relative simplicity, reference ellipsoids are used as a preferred surface on which geodetic network computations are performed and point co-ordinates such as latitude, longitude and elevation are defined.

Figure 3.8 Relationship between reference spheroid and geoid
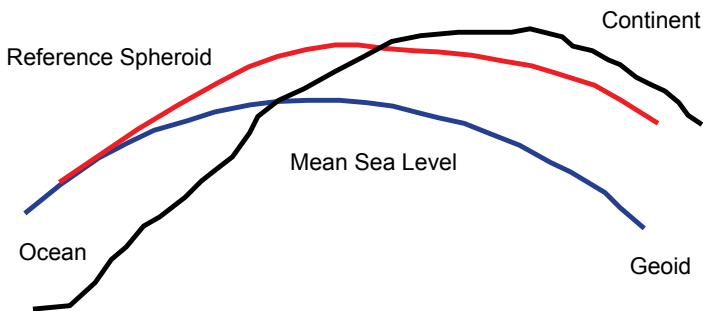
Numerous gravity points are used to calculate a mathematical relationship that approaches the real surface theoretically; for example, the International Gravity Standardisation Network of 1971 (I.G.S.N.71). The theoretical *g* of the reference spheroid can be calculated by a

summation of trigonometric functions. The theoretical g at a specific latitude φ is given by:

$$g(\varphi) = a_0 + a_1 \sin^2(\varphi) + a_2 \sin^2(2\varphi) + \ldots + a_n \sin^2(n\varphi) \qquad \text{(3-4)}$$

where $g(\varphi)$ = gravity at a specific latitude, φ = latitude and $a_0 \ldots a_n$ are constants. The constants a_i get small very quickly so only the first three terms are used when you calculate theoretical g at specific latitude. These constants are a_0 = value of g at the equator (9.7803180 m/s^2), a_1 = 0.051859158 m/s^2 and a_2 = -0.000056726 m/s^2. This calculation is called the theoretical gravity value and takes care of the latitude correction as well. The value is in m/s^2 and we express gravity in mGal. To convert these values to mGal you should multiply the value by 100 000. **Equation 3-4** then reduces to:

$$g(\varphi) = 9.7803180 + 0.051859158 \sin^2(\varphi) - 0.000056726 \sin^2(2\varphi) \qquad \text{(3-5)}$$

g at the equator is 9.7803180 m/s^2 or 978.03180 cm/s^2 (Gal) or 978031.800 milligal. Before g values at various points can be compared, they need to be reduced to a common elevation datum – the geoid.

Survey strategies

Gravity measurements are made in much the same way as magnetic surveys; that is, surveys either take the form of individual linear profiles, or grids of closely-spaced profiles. In the case of regional gravity surveys it is common to locate gravity stations along existing roads[28]. Since gravity measurements 'drift' over time, it is also standard practice to repeat the measurements at certain gravity stations every 1–2 hours and to construct a time-dependent drift-curve that can be used to correct the field data accordingly.

Gravity measurements must undergo a number of corrections and reductions before they can be ascribed primarily to the subsurface target(s) of interest:
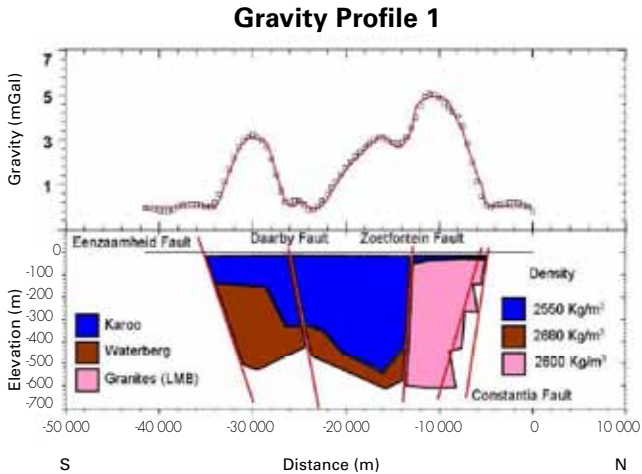
- ■ **Latitude** – the change in g due to a north-south difference in latitude (ϕ) is approximately 0.081 sinϕ g.u. per 10 m;
- ■ **Topography** – required when individual stations are located on topographic irregularities. The method is a graphical one using a topographic map of the survey area. More details can be found in Parasnis (1972)[28];
- ■ **Material between stations (Bouguer correction)** – accounts for the additional attraction of the rock mass between stations with different elevations. If the density of the intervening material is ρ, then the correction is approximately 0.4191ρ g.u. per vertical metre;
- ■ **Elevation ('free air correction')** – this equates to approximately 3.086 g.u. per metre of elevation relative to the survey datum level;
- ■ **Tidal correction** – the tides cause changes of several g.u. in the course of a day. This is usually accounted for by recording the 'drift' of the instruments over time (using a base station which is frequently revisited during a survey).

Following all the above corrections, the resulting gravity value is called the Bouguer anomaly, and represents the response of the localised subsurface density anomalies.

Link between gravity measurements and Earth parameters

Gravity data representation and interpretation is similar to that for magnetic data. Formulas for calculating the responses of various basic target shapes (e.g. horizontal cylinder, vertical cylinder, rectangular prism, etc.) can be found in the literature. Computer algorithms can also be used to perturb the properties of such targets and their surroundings (density, target geometry and depth) to model the observed field observations. Automatic iterative optimisation algorithms (referred to as 'inversion' algorithms) are commonly used for this purpose.

Figure 3.9 shows a local field example of how accurate knowledge of the densities of the various rocks in the Waterberg coalfield was used to interpret observed gravity variations in terms of structural features and regional geology[29]. **Figure 3.10** illustrates the use of a two-dimensional Bouguer map for the same purpose, but on a regional scale.

Figure 3.9 Example of a one-dimensional gravity profile over structural features in the Waterberg coalfield[29]

Figure 3.10 Example of a two-dimensional gravity (Bouguer) contour map for the Waterberg coalfield[29]
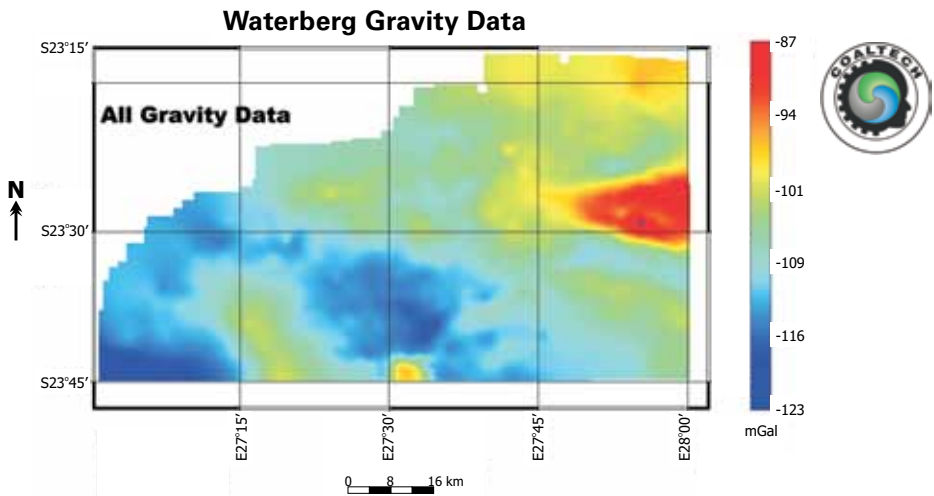
► Electrical methods (resistivity and induced polarisation)

The previously discussed methods (magnetics and gravity) both rely on natural potential fields. The electrical methods described in this section rely on an artificial source, namely a direct current (or a low-frequency alternating current) injected into the portion of Earth being investigated.

The physical property of **resistivity** relates to the way in which a material conducts electrical charge, while the **polarisability** (or chargeability) relates to the way in which the material stores charge. These physical properties of geological materials are controlled by factors such as porosity, degree of saturation, conductivity of the pore fluid, shape and distribution of pore spaces, the texture of the material, and the presence of conductive constituents such as sulphides, oxides and clay particles. The resistivity method is used to map spatial variations in subsurface electrical resistivity (reciprocal of conductivity), while the induced polarisation (IP) method is used to map variations in chargeability.

The conventional (DC) resistivity method has been around for approximately a century, and resistivity profiling and soundings have been applied extensively across South Africa, including the coal mining areas. In the last couple of decades, the method has undergone a major revolution, brought about by rapid advances in electronic hardware, computer technology and modelling approaches. Consequently, there are major differences in the way that the resistivity method is commonly applied today:

■ The move to an **imaging** or **tomographic** approach – the concepts of traditional one-dimensional (depth) soundings and two-dimensional profiling are combined; large multi-channel data sets and modern algorithms enable data to be converted to true resistivity-depth images, unlike the approximate depth models formerly derived from graphical plotting methods

■ The joint use of resistivity and induced polarisation (IP) – modern commercial resistivity systems allow the simultaneous recording of resistivity and IP data, since the two methods use the same data acquisition configurations and measurement schemes. As one might expect, the combination of these methods offers better discrimination than either of the individual methods alone.

Conventional depth sounding and profiling approaches may still be useful in some cases, but they are outdated. One can nowadays acquire large tomographic data sets, including both resistivity and IP data, with modern multi-channel acquisition systems with more or less the same effort that was formerly required to conduct a single Schlumberger sounding or a few two-dimensional (cross-sectional) resistivity profiles. The modern methods are therefore strongly recommended.

Fundamental principles

The resistivity and IP methods are based on the phenomena of **conduction** and **polarisation**. For more detailed discussions of these and related aspects, or of the methods in general, the reader is referred to any of the listed general reference books on this subject[24, 30-35]. This section on fundamental principles will instead focus on the relationship between the measured and derived resistivity and IP parameters.

In resistivity surveys, the transmitter typically generates a series of current pulses with alternating polarity (**Figure 3.11**) and a cycle period of a few seconds. A resistivity measurement involves averaging the current and resulting voltage over several current inversion cycles to reduce unwanted electrode polarisation effects and to improve the signal-to-noise ratio[30, 33]. For measurements, four galvanic electrodes are generally used: one pair for current injection and one pair for recording the voltage. If electrical resistivity is the only property of interest, it is only necessary to record the steady-state current and voltage values. However, the IP method can be implemented concurrently with the same equipment, as the method exploits the earth's dynamic response to the abrupt termination of the source current described above – in other words, during the off times depicted in **Figure 3.11a**.

Figure 3.11 Typical DC current source and corresponding Earth voltage response

(a)

(b)
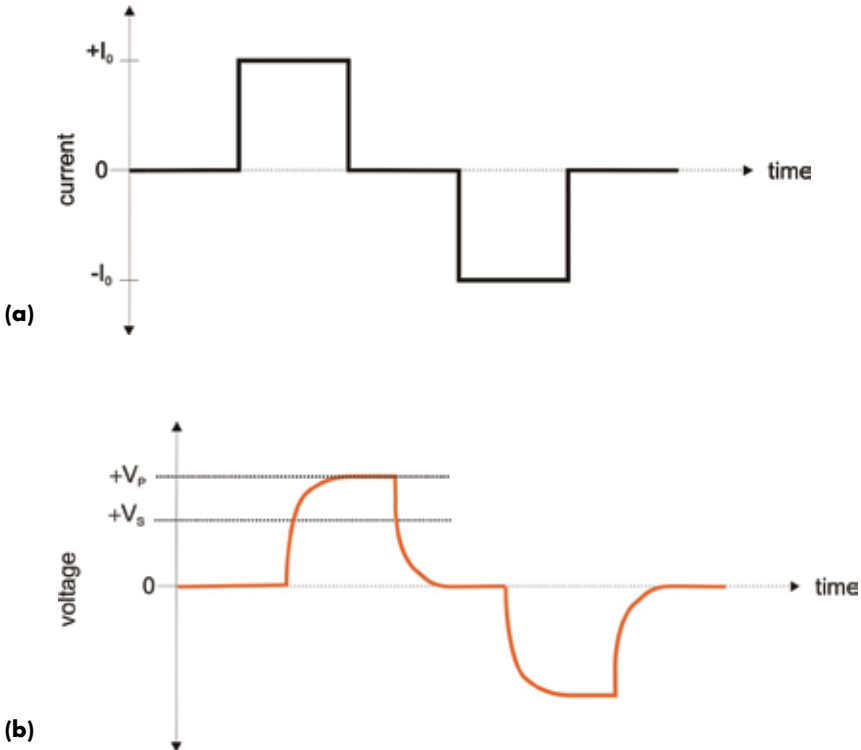
When the current is switched off, the observed voltage does not instantaneously drop off to zero, but exhibits a transient decay (**Figure 3.11b**). The IP parameters are normally derived from this portion of the voltage curve – this approach is referred to as the **time-domain** IP approach. IP measurements can also be conducted in the frequency domain[32, 36], where the variation in resistivity with the source frequency is observed; this is equivalent to determining the phase difference between the current and the measured voltage, if we describe these quantities using complex numbers.

Units and terminology

Apparent resistivity

In conventional resistivity prospecting the parameter usually derived from the field measurements is apparent resistivity, defined as[24, 32, 33]:

$$\rho_a = \frac{K \, \Delta V}{I} \tag{3-6}$$

where K is the geometric factor and is derived from the positions of the four electrodes A, B, M and N. ρ_a will only equal the true resistivity of the Earth for an electrically homogeneous Earth (no subsurface resistivity variations). In practice, ρ_a should be regarded as a semi-quantitative parameter to assess the extent to which some Earth model differs from a homogeneous Earth model.

Chargeability (m)

This time domain IP parameter was introduced by Seigel in 1959[32] and is the ratio of the secondary voltage V_s (attained immediately after current termination) to primary voltage V_p (attained just before current termination):

$$m = \frac{V_s}{V_p} \tag{3-7}$$

Since V_s used to be difficult to measure in practice, the average or integral chargeability has traditionally been used:

$$M = \frac{1}{(t_2 - t_1) V_p} \int_{t_1}^{t_2} V(t) \, dt \tag{3-8}$$

where t_2-t_1 represents an appropriate, but somewhat subjectively-chosen time window along the voltage decay curve. Newmont-type IP receivers typically use a time window between 0.45 s and 1.1 s within a 2 s switch-off time[37]. The unit of chargeability is *mV/V*, or may be expressed as a percentage.

Resistivity magnitude and phase (complex resistivity parameters)

As previously mentioned, an alternative method of evaluating the IP effect is to measure the phase shift between the source current and the resulting voltage waveforms. In the complex resistivity (CR) method the measured quantities are the magnitude and phase of a frequency-dependent complex resistivity; that is, $P(\omega)$ and $\phi(\omega)$. These parameters are often expressed in terms of the real and imaginary components of the complex conductivity[30, 38]:

$$\sigma^{*}(\omega) = \frac{1}{\rho^{*}(\omega)} = |\sigma|e^{i\varphi} = \sigma^{'}(\omega) + i\,\sigma^{''}(\omega) \tag{3-9}$$

σ^{*} and P^{*} are the complex conductivity and complex resistivity, respectively;
ω is the frequency;
σ' and σ'' are the real and imaginary conductivities, which represent the conduction and polarisation components;
$|\sigma|$ is the magnitude of conductivity; and
ϕ is the phase angle.

Frequency-domain geophysical systems, such as the Zonge GDP-32[II] multi-function receiver, typically acquire complex resistivity data as the conductivity (or resistivity) magnitude and phase angle. It is also possible to acquire IP data over a range of discrete frequencies, typically covering several decades on a logarithmic scale. This type of survey is referred to as the spectral IP (SIP) method.

Survey strategies

This section describes the basic principles of acquiring resistivity and IP field measurements and also discusses the most commonly used survey configurations and measurement schemes. Survey **configurations** or **arrays** refer to the number of electrodes and the geometrical pattern in which they are arranged, while measurement **schemes** refer to the sequence, combination and number of electrode positions used for individual measurements.

In traditional resistivity surveys, the Schlumberger, Wenner and dipole-dipole arrays were typically used. In modern imaging surveys, most practitioners prefer to use either the dipole-dipole or the pole-dipole array, and several model studies have indicated that these two arrays provide the best results. Both multiple dipole spacings and multiple dipole lengths should be used, to maximise the depth of investigation and to optimise the mapping accuracy at all depths. **Figure 3.12** illustrates these concepts for a linear, surface dipole-dipole array – a number of different arrays is in fact based on a line of several equidistant electrodes. In order to obtain both lateral and depth information, the following systematic approach or **measurement scheme** is commonly used. The first two electrode positions (1 and 2) are used as a current injection pair ($C1_1$, $C2_1$) and the resulting potential difference and IP values are recorded at several other electrode pairs ($P1_j$ and $P2_j$). The current electrodes are also often denoted by the letters A and B and the potential electrodes by M and N. If the unit electrode spacing is denoted by a, the measurements are usually recorded for increasing values of n,

where n denotes the dipole spacing expressed in multiples of a; that is, for a fixed current electrode pair, data is typically recorded for n = a, 2a, …, etc. The recorded signal strength drops off rapidly as n increases and consequently data is seldom recorded for n above 8–10. A sequence of (say) eight to ten measurements for a fixed current pair is often referred to as a **profile**. After the first profile, the current pair is moved incrementally to occupy successive adjacent locations (2 and 3, 3 and 4, etc.) and another set of 8–10 measurements is recorded in each case. This is called the 'skip 0' scheme. Once all adjacent electrode pairs have been exploited for current injection (using a dipole length equal to the unit electrode spacing a) the current and voltage dipole lengths can be increased to 2a and the above measurement procedure repeated, yielding a 'skip 1' scheme. Although a 'skip 0' scheme alone may provide adequate detection, a combination of 'skip 0' with 'skip 1' or 'skip 2' is recommended, as this provides improved resolution at greater depths.

Figure 3.12 Electrical surveying using the dipole-dipole array (top) and Wenner array (bottom)
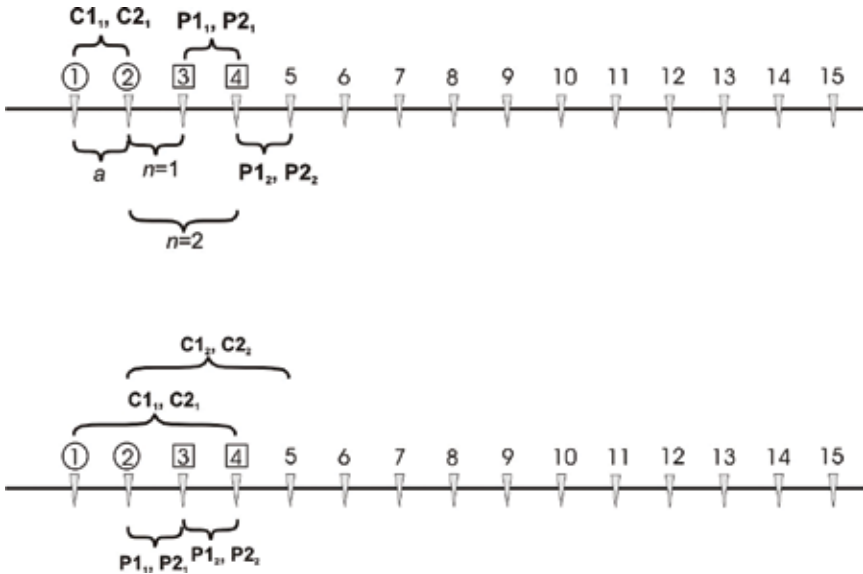
The same linear array of electrodes can also be used for the pole-dipole and Wenner approaches. The pole-dipole approach is similar to the dipole-dipole approach except that the pair of current electrodes is made to approximate a pole electrode, by embedding one current electrode (C_1) in the ground at a remote location throughout the survey. If the distance between C_1 and the survey area is at least 10–20 times the largest inter-electrode spacing, then the electrode C_2 approximates a pole electrode. As an illustration, if a unit electrode spacing of 5 m is used and data is acquired for up to n=10, the remote electrode should ideally be located at least 500 m away.

In the more traditional Wenner array, the sequence of electrodes for individual measurements is A-MN-B, instead of AB-MN as used in the dipole-dipole and pole-dipole approaches. In other words, the voltage is recorded in the centre between the current electrode pair. For any given measurement the distances AM, MN and NB are equal; that is, the whole four-electrode array is displaced by the same distance after each measurement. So, for a unit electrode spacing, the first measurement might involve electrodes 1 and 4 for current injection and electrodes 2 and 3 for voltage measurement. The second measurement would then involve electrodes 2 and 5 (current injection) and 3 and 4 (voltage measurement), respectively, and so on. This incremental lateral movement of the four-electrode array provides information about the lateral variations in subsurface electrical properties. By repeating the process for different values of the inter-electrode spacing, depth-varying information can be added to the data set.

The preceding discussion on survey strategies has focused primarily on surface surveys. When boreholes are available, the optimum choice of measurement array and measurement scheme is less straightforward; the geometry of the effective survey area and the expected target should be considered. For example, a single borehole may be combined with a line of surface electrodes to yield an effectively triangular survey area. In cases where two or more boreholes are available, significantly different survey geometries may result (Figure 3.13).

It is strongly recommended to use computer simulations to find an appropriate measurement configuration and scheme before embarking on such field surveys. In practice, a combination of in-line (e.g. along individual boreholes or surface line) and cross-line (e.g. borehole-to-borehole and borehole-to-surface) dipole-dipole measurements usually provides reasonable imaging results.

Figure 3.13 Schematic illustrating how two vastly different survey area geometries might result when exploiting boreholes in resistivity/IP surveys
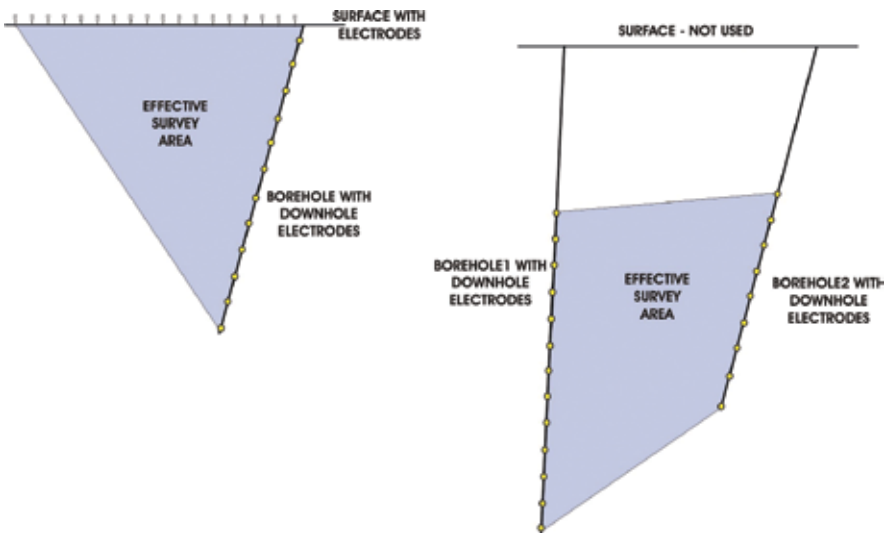
Link between resistivity/IP measurements and Earth parameters

In this section, a simplified computer simulation is used to compare the typical outputs of traditional versus modern resistivity-based survey approaches and to demonstrate the link between field measurements and Earth parameters. **Figure 3.14a** depicts an Earth model in which two targets (A and B) and a layer boundary occur. Target A is five times more conductive than its surroundings and also has a similar IP contrast (expressed here as a complex resistivity phase angle). Target B, however, has a higher IP contrast of approximately 8:1 with its hosting layer. The basement has a moderate resistivity contrast with the upper layer (3:1), but the contrast in polarisability is very subtle (< 2:1).

    Figure 3.14b shows a classic Schlumberger sounding curve calculated over the central part of the model. **Figures 3.14c** and **3.14d** show the outputs from constant depth dipole-dipole profiling surveys (showing resistivity magnitude and IP phase angle). **Figure 3.14e** shows the ERT and associated IP tomography images that can be simultaneously derived from a dipole-dipole data set involving multiple dipole length and multiple dipole spacing measurements.

Figure 3.14 Comparison of traditional and modern resistivity and IP survey outputs – a model study demonstration

(a) *Geoelectric model with a conductive and polarisable target block A in the upper layer and a polarisable target B in the basement layer*
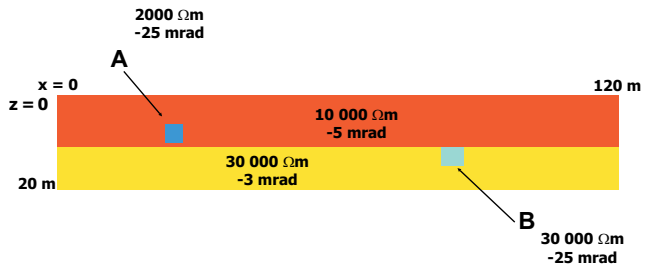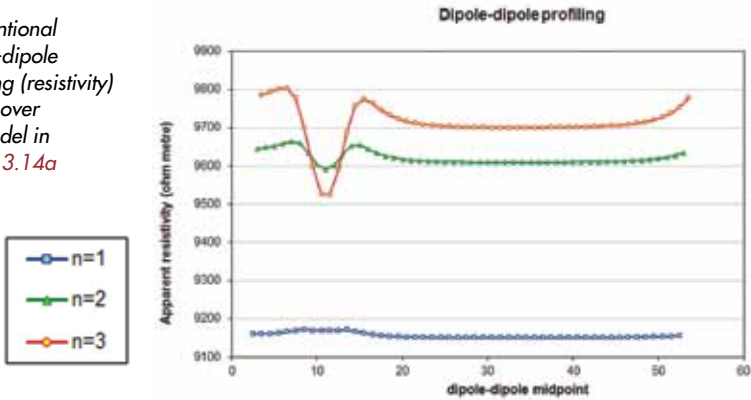

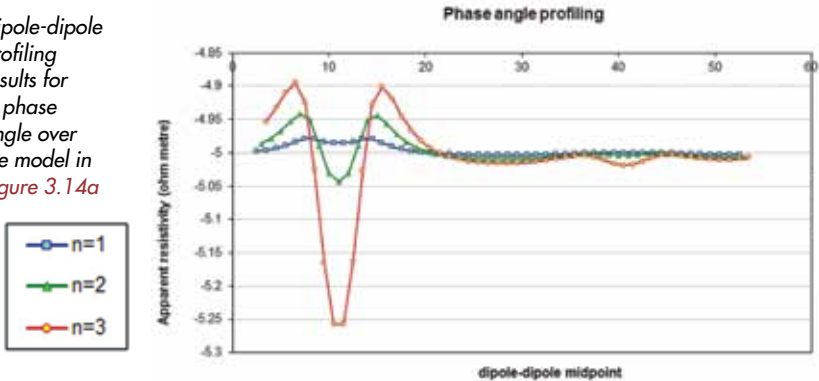**(b)** *Conventional DC Schlumberger sounding results over the model in Figure 3.14a*

(c) *Conventional dipole-dipole profiling (resistivity) results over the model in* *Figure 3.14a*

Dipole-dipole profiling

(d) *Dipole-dipole profiling results for IP phase angle over the model in* *Figure 3.14a*

Phase angle profiling

(e) *ERT and IP tomography reconstructions of synthetic model response*
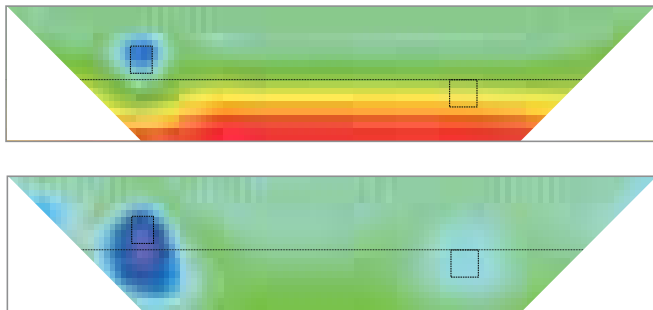
The Schlumberger sounding, which was centred at x = 60 m, only reveals the presence of a 2-layered Earth. Even though a quantitative depth-to-basement can be determined with reasonable accuracy from such sounding curves, the sounding method cannot be used to

detect the smaller isolated anomalies. The profiling approach does manage to detect target A for both resistivity magnitude and IP phase angle. The subtle IP anomaly of target B is, however, masked by the more prominent response of target A, which not only has a greater property contrast with its surroundings, but is also much shallower and therefore easier to detect. Target B hardly manifests on the phase-angle profiles. One further limitation of the profiling results is that only semi-quantitative information about the detected targets can be estimated – the true depth and geometry cannot be derived from such results.

The imaging results shown in Figure 3.14e provide a lot more quantitative information. By jointly considering the ERT and IP tomography output images, one is able to infer the presence of the layer boundary as well as the two targets, A and B.
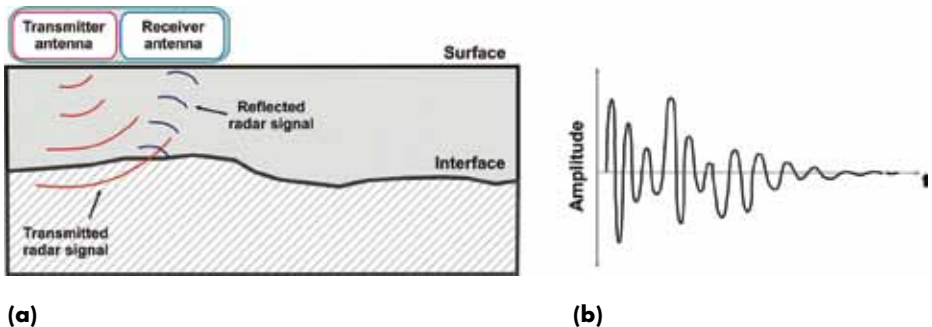
▶ Ground-penetrating radar (GPR)

Ground-penetrating radar (GPR) has a poor track record and reputation in the South African coal mining industry. GPR has been applied in both surface and underground environments, particularly in the Witbank coalfield, but results have generally been disappointing. The method should nevertheless not be disregarded completely as it may have some niche applications in coal mining and exploration. Furthermore, hardware and processing technologies have improved significantly since the early commercial GPR systems were tested in South African coal mines and perhaps a comprehensive re-evaluation of the method, its capabilities and limitations is required. GPR is relatively easy and inexpensive to apply and is used as a routine rock engineering tool (hangingwall investigations for support design) in other commodities; for example, in some of the local platinum and chrome mines. A brief overview of the method follows.
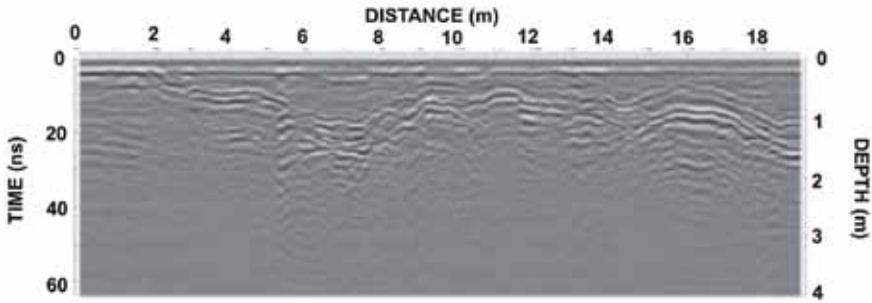
Fundamental principles

In a typical GPR system, a radar pulse is transmitted into the Earth and any reflections off interfaces or objects in the Earth are detected by a receive antenna (Figure 3.15a)[39].

Figure 3.15 Schematic depicting GPR system and data representation

(a)

(b)

(c)

The recorded signal from a single transmitter position is called a trace (**Figure 3.15b**), and shows the received signal amplitude as a function of time. A GPR data set or **radargram** (**Figure 3.15c**) usually comprises a sequence of closely spaced traces along a line or profile. A GPR image or radargram is very similar to a seismic record or seismogram; the vertical axis represents the two-way travel time of the radar signal and the horizontal axis indicates the position of the antennas along the radar profile. The travel time is usually converted to an equivalent depth for display purposes. Reflections within the subsurface are typically represented as variations in a grey display scale.

Two electrical properties dictate the applicability and performance of GPR[39, 40]: The dielectric constant or **permittivity** determines whether a layer or object will reflect the transmitted signal. The signal penetration, and therefore the effective range of GPR, is however controlled mostly by the electrical **conductivity** of the host rock. Radar signals are attenuated in rock and the attenuation increases with increasing conductivity and operating frequency, resulting in decreased radar penetration and shorter ranges. Resistive host rocks like quartzite, lava, anorthosite, etc. are, for example, better radar environments than more conductive dolomites, shales and sandstones. There is a trade-off between range and resolution (mapping accuracy). The lower the operating frequency, the less the attenuation and the better the range; however, by lowering the frequency one also decreases the resolution. Noon (1996) presented a convenient way of estimating GPR performance, which is based on the loss tangent of the host rock. The effective loss tangent combines the above two properties and, for lossy dielectrics, is defined as:

$$\tan\delta = \frac{\sigma_e}{\omega\varepsilon_e} = \frac{\sigma}{\omega\varepsilon_r\varepsilon_0} \tag{3-10}$$

where σ_e is the effective real conductivity, ε_e is the effective real permittivity, ε_r is the relative permittivity, $\varepsilon_0 = 8.854 \times 10^{-12}$ and $\omega = 2\pi f$. **Figure 3.16** shows a series of nomograms for different loss tangent values. The vertical axis of the graph plots the losses (in dB) that a GPR system can tolerate before signal-to-noise becomes too high for effective operation; the horizontal axis shows the range or penetration in terms of wavelengths.

To illustrate the meaning and use of the loss tangent nomograms using typical property values, refer to Table 3.2. The penetration values in the table were read off the nomograms by making the realistic assumption that a typical commercial GPR system can tolerate losses of up to 120 dB.

This example illustrates how, with the same GPR system, one can achieve a depth of investigation of up to 8 m at one site, while at another site it is almost impossible to 'see' beyond 1 m.

Figure 3.16 Nomograms that show the relationship between maximum range, resolution and the loss tangent of the host rock[41]

Smooth Planar Reflector
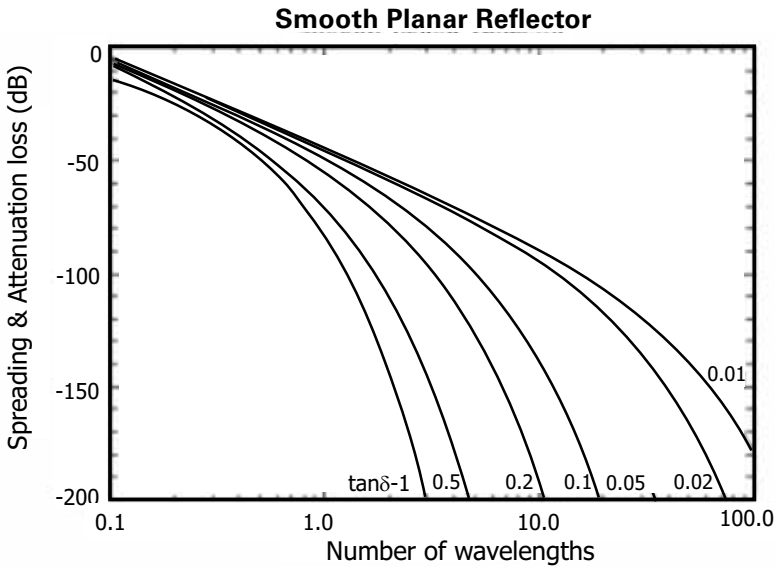
Table 3.2 Typical performance figures for GPR in different host environments

f=500 MHz; $\varepsilon_r = 9$	RESISTIVITY (Ωm)	LOSS TANGENT	PENETRATION (WAVELENGTHS)	WAVELENGTH (m)	PENETRATION (m)
Dry, hard rock	2 000	0.002	30–40	0.2	6–8 m
Overburden/ top soil	200	0.02	~ 20	0.2	~ 4m
Graphitic shale	20	0.2	~ 5	0.2	~ 1 m

Figure 3.17 Examples of commercial GPR systems configurations

(a)

(b)

Survey strategies

The typical modern GPR system comprises a fixed-frequency transmitter and receiver packaged together into a single unit. GPR systems can be configured to be used either on the Earth's surface or in underground mines. For example, **Figure 3.17a** shows a 250 MHz **Rock Noggin** GPR system mounted on a cart for surface profiling; **Figure 3.17b** shows a portable 500 MHz **Rock Noggin** configured for one-man, in-mine operation.

When planning a GPR survey, the user generally has to select a number of important survey parameters. These include the operating frequency, the range of interest and the survey design; that is, the direction, length, number and spacing of the profiles.

Operating frequency, range and resolution

The choice of antenna frequency is determined mainly by the scale of the target (size and depth) to be detected and the desired range. The range-resolution trade-off can be controlled to some extent by the operator: the higher the frequency, the shorter the wavelength and the better the resolution (smaller target features can be resolved); however, due to the associated higher attenuation the effective operating range is also reduced. Lowering the frequency does provide a better operating range, but since the radar wavelength is longer, the resolution decreases accordingly. **Table 3.3** compares the typical performance of two different frequencies in a resistive environment. Since GPR antennas for geological applications are available for frequencies ranging from approximately 200 MHz to 1 000 MHz, two extremes are compared:

Table 3.3 GPR performance parameters for different frequencies

FREQUENCY (MHz)	WAVELENGTH (m)	RANGE (m)	TYPICAL APPLICATION
200	~ 0.5	6–12 m	Detecting layer boundaries located several metres below surface or into the hangingwall or roof
1 000	~ 0.1	2–3 m	Assessment of fracture characteristics in the immediate hangingwall, roof or sidewall

Note: *The above estimates are typical for a resistive hard rock environment such as the Bushveld Complex or Witwatersrand Basin. In South African coal mines, however, the effective ranges are expected to be significantly lower due to the relatively conductive nature (higher loss tangent) of in situ coal and associated sandstones, shales etc.*

Many GPR practitioners involved in mining applications prefer to use a system in the frequency band 400–500 MHz as this provides a good compromise between range and resolution, which can be used to address a wide range of problems.

Survey design

The geometry of the target and the available access dictate the optimum survey layout. In the simplest case, the problem may involve a linear target feature with the strike more or less known; for example, locating the surface position of a known fault or intrusive dyke. In such a case, a simple linear GPR profile that crosses the expected feature more or less perpendicularly is required. If the extent of the feature needs to be extrapolated or tracked along strike, several parallel GPR profiles will be required. The problem of specifying a survey layout becomes more complicated if the target is relatively small and isolated, or its geometry or location is not well known[39]. In such cases it may be necessary to acquire many GPR profiles in different directions across the area of interest – a so-called grid survey. For the detailed subsurface mapping of an area the three-dimensional GPR approach is sometimes used. This involves covering an area with a dense grid of closely-spaced profiles, usually in two perpendicular directions. All the resulting data is then used as input to special three-dimensional visualisation software that displays the data in a single three-dimensional view that can be rotated or sliced to focus on specific sub-regions or planes of interest.

An important concept in survey design for any profiling method is that of **sampling rate**. In GPR surveys, if the in-line station spacing (trace interval or Δx) or the interval between successive measurements in time (time interval or Δt) is too large, then certain target features may not be detectable. The same applies to grid surveys and the spacing between adjacent profiles (line spacing or Δy). Using too coarse a sampling rate is like trying to catch small stones in a sieve that has holes bigger than the stone diameters. More details on how to optimise the survey design, in terms of resolution limits and sampling theory, can be found in Annan (2009), but the following rules of thumb can be applied[40]:

- In-line sampling interval (Δx) should ideally be ~ ⅓ of the radar wavelength;
- Time-interval (Δt) should ideally be f/3.

Referring to the examples in **Table 3.3**, the ideal maximum values for Δx and Δt are given in **Table 3.4**.

Fortunately, the default settings of most modern commercial GPR systems will automatically ensure that these sampling

Table 3.4 GPR survey design parameter examples

FREQUENCY (MHz)	WAVELENGTH (m)	Δx	Δt
200	~ 0.5	≤ 16 cm	≤ 0.66 ns
1000	~ 0.1	≤ 3 cm	≤ 0.66 ns

requirements are met. But in grid surveys, the line spacing (Δy) must still be selected. Ideally, Δy should equal Δx, but for economic and logistical reasons this requirement is often relaxed. In practice, one chooses the line spacing such that at least two profiles will cross the estimated target[39].

Typical GPR processing stream

GPR datasets are subjected to a series of basic processing steps aimed at enhancing the reflections of interest and suppressing unwanted features in the data, including noise and reflections from non-target features. The standard filters applied to 'raw' GPR data include a dewow filter, a bandpass filter and some kind of gain function. The first two filters suppress responses far from the operating frequency of the system while the gain filter preferentially amplifies deep reflections, which suffer more attenuation than echoes from shallow targets.

Most modern GPR systems offer real-time data visualisation wherein a pre-defined sequence of standard processing filters is applied as the data is acquired. This enables operators to see target responses as the survey proceeds. However, real-time filtering is often not effective in identifying subtle target features, and survey production constraints may not allow detailed in-field analyses; in such cases it is standard procedure to conduct post-survey processing.

Link between GPR measurements and Earth parameters

The radargrams presented in Figure 3.18 illustrate how effective GPR can be in the right conditions. Figure 3.18a shows the result from a hangingwall investigation in a local platinum mine. Here the primary target was a prominent chromitite stringer approximately 1.2 m up into the hangingwall. The corresponding target reflection can be clearly seen on the

Figure 3.18a GPR output examples
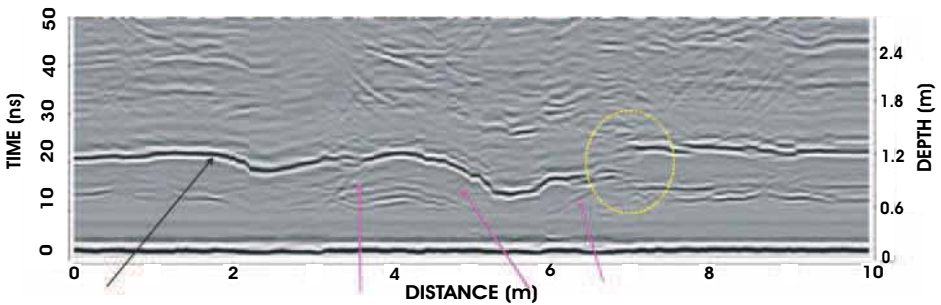
Figure 3.18b GPR surface utility mapping
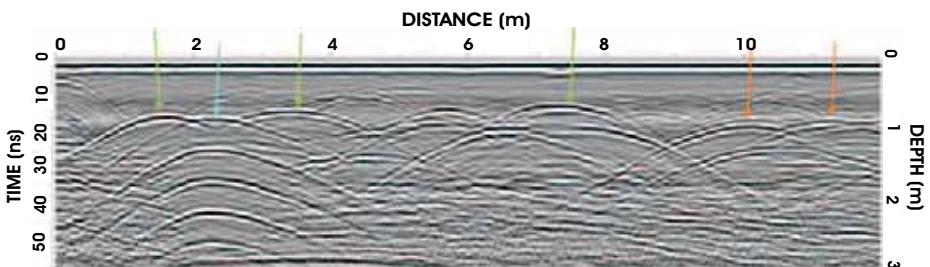
radargram (black arrow) and an apparent vertical displacement of the layer can be seen at x = 7 m (yellow dotted ellipse). More subtle structural features in the form of possible angled joints can also be seen at x = 3.3 m, x = 5 m and at x = 6.5 m (magenta arrows).

The radargram in **Figure 3.18b** is from a surface utility mapping study. In contrast to the linear target features in the previous example, localised targets (or linear features that are traversed perpendicularly) respond like point reflectors, i.e., they manifest as hyperbolic reflections on a radargram. In this particular example the observed anomalies could be correlated with known water pipes (cyan arrow), electrical and telecommunication cables (orange arrows) and shallow tree roots (green arrows).

▶ Frequency-domain electromagnetic method (FDEM)

Frequency-domain electromagnetics (FDEM) is a popular, general purpose geophysical mapping tool, because it is relatively easy and inexpensive to apply. It is well-suited to detecting and mapping conductive target features in the upper 40–50 m and is often used as a complementary tool to the magnetic and gravity methods. Typical applications include the mapping of lateral transitions in soil/rock type, contaminant plumes, saline intrusions, sand and gravel deposits and clay aquitards, and for shallow bedrock investigations and the detection of buried pipes and metal objects[42, 43]. It may also be applicable to the mapping of near-surface cavities[44].

Fundamental principles

In FDEM surveys a transmitter (Tx) coil and receiver (Rx) coil are used in tandem (**Figure 3.19**). The two coils are typically placed on the ground some distance apart, in either a horizontal dipole mode (coils coplanar and vertically orientated) or in the vertical dipole mode (coils coplanar and horizontally orientated). An EM signal is transmitted at a fixed frequency by the Tx coil, which induces eddy currents in the subsurface. These eddy currents then generate a secondary magnetic field, which is recorded by the Rx coil. The mutual inductance between the Tx and subsurface conductors is described by a complex quantity and, consequently, the secondary field will have an associated phase shift[45].

The measured field contains a primary field contribution, which is normally compensated for during the measurement process. Some FDEM systems record the amplitude and phase components of the (complex) secondary field. Others record the in-phase (real) and quadrature (imaginary or out-of-phase) components of the secondary field. These secondary field components provide distinctive clues about subsurface conductors: The quadrature component can be converted to a measure of apparent ground conductivity; that is, the average conductivity down to the depth of investigation for the specific system configuration. The in-phase field component is less responsive to variations in bulk conductivity, but is fairly sensitive to highly-conductive bodies such as metal objects.

In FDEM surveying, the depth of investigation can be controlled by changing the Tx frequency: the lower the frequency, the greater the penetration of the primary field into

the Earth, and hence, the greater the depth of investigation. Some FDEM systems only have two or three frequencies to select from, while others offer a range of discrete frequencies. The operating frequency is usually associated with a fixed coil spacing and these parameters imply an approximately fixed depth of investigation[44]. Where depth (sounding) information is required at a given measurement position, it is necessary to exploit several different frequency and dipole mode combinations.

Figure 3.19 Schematic illustration of the principles of FDEM method[43]
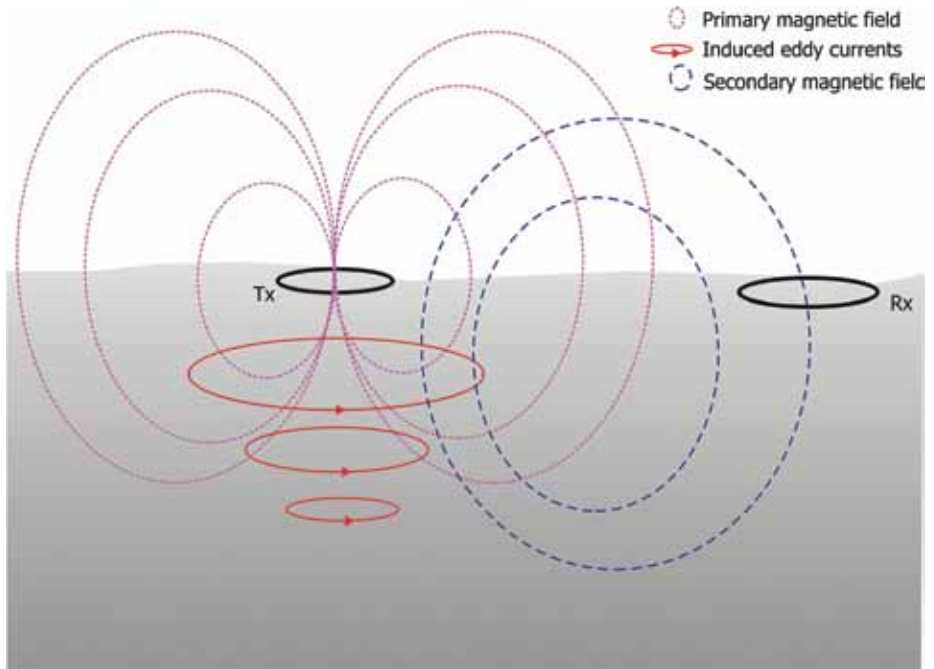
Survey strategies

As mentioned earlier, in FDEM surveying the user has some flexibility in terms of coil orientation, operating frequency and coil separation. The optimum combination of these survey parameters is dictated largely by the purpose of the survey, the characteristics of the target and the desired depth of investigation. The depth of exploration, for example, is determined by the transmitter-receiver separation and the orientation of the transmitter and receiver coil axes[43]. However, to extract the maximum information from the ground in a survey, EM practitioners typically exploit multiple combinations of coil orientations and discrete operating frequencies and/or intercoil spacings. For example, with the well-known Geonics EM-34 system (**Figure 3.20a**), two conventional coil orientations are possible (vertical and horizontal), and three different frequencies are available (6.4 kHz, 1.6 kHz and 0.4 kHz),

each associated with a fixed coil spacing (10 m, 20 m and 40 m). In contrast, the Geonics EM-31 (**Figure 3.20b**) can be operated in either vertical or horizontal dipole mode, at a single frequency of 9.8 kHz, with a fixed coil spacing of 3.66 m. The more versatile EM-34 therefore allows six different measurements and can achieve penetration depths of several tens of metres. With the EM-31, only two different measurements are possible, and the higher operating frequency and smaller coil spacing only enable penetration of a few metres.

When analysing data sets, particularly where time or other constraints have only allowed for acquisition using a single coil orientation, it is useful to be aware that the vertical dipole mode is fairly sensitive to steeply dipping conductive targets, while the horizontal dipole mode is relatively insensitive to such targets, but is well suited to providing a good estimate of the bulk ground conductivity.

When conducting FDEM profiles, a station spacing of between a third and a half the intercoil spacing is recommended to ensure adequate resolution. In some cases, a few individual FDEM profiles may provide sufficient information about the target; for example, locating the edge of a thin dyke or a fault. More often than not, however, the user is interested in the extent or trend of conductive targets and then has to resort to two-dimensional surveys; that is, a grid of closely spaced parallel profiles over the area of interest.

FDEM instruments typically record conductivity values in mS/m: 1 mS/m is the same as 1 000 Ωm, which is moderately resistive in geoelectric terms. Conductive ground will have a higher conductivity, say 10 mS/m, for which the resistivity equivalent is 100 Ωm.

Figure 3.20 Examples of typical commercial FDEM systems in operation
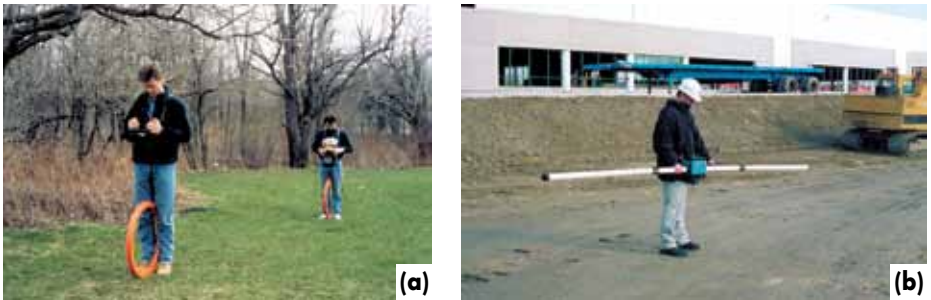
*A Geonics EM-34 being employed in horizontal dipole (vertical loop) mode **(a)**, and a Geonics EM-31 system **(b)**. (Pictures courtesy of Geonics Limited)*

Link between measured and Earth parameters

To understand the relationship between observed FDEM parameters and Earth parameters, the concepts of 'skin effect' and 'skin depth' are important. Skin effect is the tendency of an alternating electric current density to be largest near the surface of the conductor, and to decrease deeper in the conductor. The electric current flows mainly at the 'skin' of the conductor, between the outer surface and a level called the skin depth. The skin depth is

defined as the depth at which the amplitude of a plane wave has decreased to 1/e or 37% of its initial amplitude. Skin depth is approximated by the formula:

$$\delta = \sqrt{\frac{2\rho}{\omega\mu}}$$

(3-11)

ρ = resistivity of the conductor
ω = angular frequency of current = $2\pi \times$ frequency (f)
μ = absolute magnetic permeability of the conductor

The skin effect explains the limited depth of investigation in some surveys. The more conductive the ground, the smaller the skin depth and the depth of investigation; increasing the frequency also decreases the depth of investigation.

The subsurface conductivity can be affected by the following factors:

- Mineral composition of layers/structures
- Presence of clay
- Moisture content
- Porosity
- Conductivity of groundwater
- Presence of contaminants in the ground

As was pointed out in Chapter 2, the conductivity of geological materials can vary over large ranges and these ranges overlap for different rock types (refer to **Figure 2.1**). High-conductivity environments (e.g clay-rich soils) hinder effective FDEM prospecting. FDEM performs better in low-conductivity environments (e.g. loose sands, sandy soils and hard rock environments). The conductivity ranges for some rock types commonly found in South African coalfields, e.g. sandstone, limestone and till, extend to both extremes of the conductivity scale, making the applicability of FDEM unpredictable and site-specific.

Figure 3.21 Comparison of relative contribution of FDEM dipole modes as a function of depth; after McNeill (1980)[42]
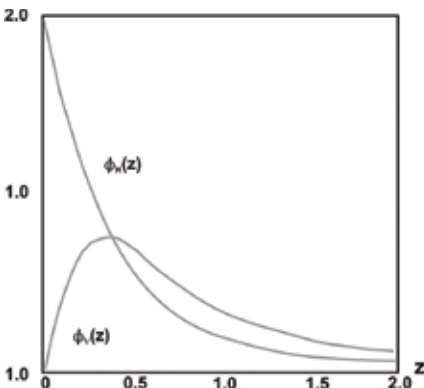
The relative responses of the dipole modes are also important. **Figure 3.21** shows the dipole response as a function of normalised depth (depth/coil spacing). The horizontal dipole is far more sensitive to near-surface conditions, while at depths exceeding one intercoil spacing the vertical dipole contribution is significantly larger.

Another useful number that helps us to better understand the FDEM response is the so-called **response parameter**, defined as the

product of conductivity-thickness (σt), permeability (μ), angular frequency ($\omega = 2\pi f$), and the square of some mean dimension of the target (a^2)[45]. **Figure 3.22** shows a plot of the relative in-phase and out-of-phase response function versus the response parameter defined above for a conducting sphere target in a uniform field background. For low values of the response parameter (< 1), the sphere will generally produce a low-amplitude out-of-phase anomaly; at moderate values of the response parameter (10–100), the response will be a moderate-amplitude in-phase and out-of-phase anomaly, whereas for high values of the response parameter (> 1,000), the response will usually be in the in-phase component. In FDEM, the depth and size of the conductor primarily affect the amplitude of the secondary field, while the conductivity of the target mainly affects the ratio of in-phase to out-of-phase amplitudes[45].

Figure 3.22 Comparison of in-phase and out-of-phase response as a function of the response parameter
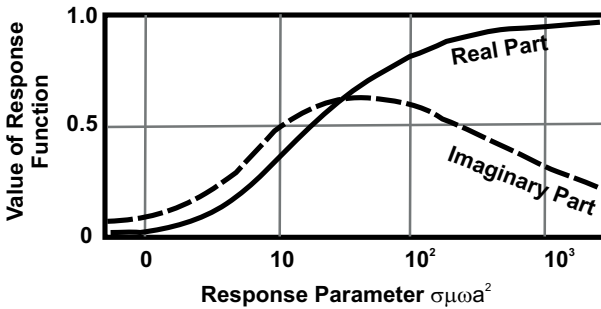
Operation at low induction numbers

The final basic concept explained here is the so-called 'operation at low-induction numbers', which is implemented in many commonly used FDEM systems that can be described as terrain conductivity meters.

FDEM receiver coils essentially record the ratio of the secondary magnetic field H_S to the primary magnetic field H_p. The mathematical expressions for this ratio (for the respective dipole modes) are complicated functions of frequency and conductivity. If the so-called induction number (ratio of coil spacing to skin depth) is << 1 (the coil spacing is much less than the skin depth), then the magnitude of the secondary field H_S is directly proportional to the ground conductivity and the phase of H_S leads H_P by 90 degrees. This also means that the apparent conductivity recorded by the instrument then reduces to[42]:

$$\sigma_a = \frac{4}{\omega \mu_0 s^2} \left(\frac{H_s}{H_p} \right)_{\substack{quadrature \\ component}}$$

(3-12)

Survey output examples

Unless single point anomalies are sought, FDEM data sets are acquired using a two-dimensional approach as described under Survey strategies on page 58. The measurements are then geo-referenced and contoured as one would do with other potential field data sets such as magnetic or gravity data. **Figure 3.23** shows some examples of typical FDEM survey outputs. In the top image is an apparent conductivity profile acquired over a fault zone that has been intruded by saline water, making it a good EM target[46]. The image in the middle shows how helicopter-based FDEM was used to map acidic plumes over coal mine spoils in Pennsylvania, USA[47]; a two-dimensional cross-sectional output or conductivity-depth image (CDI) is shown. The bottom image shows a two-dimensional plan contour map of near-surface conductivity values. The purpose of this survey was to map spatial variations in soil conductivity caused by high salinity anomalies[48].

Figure 3.23 Examples of typical FDEM outputs
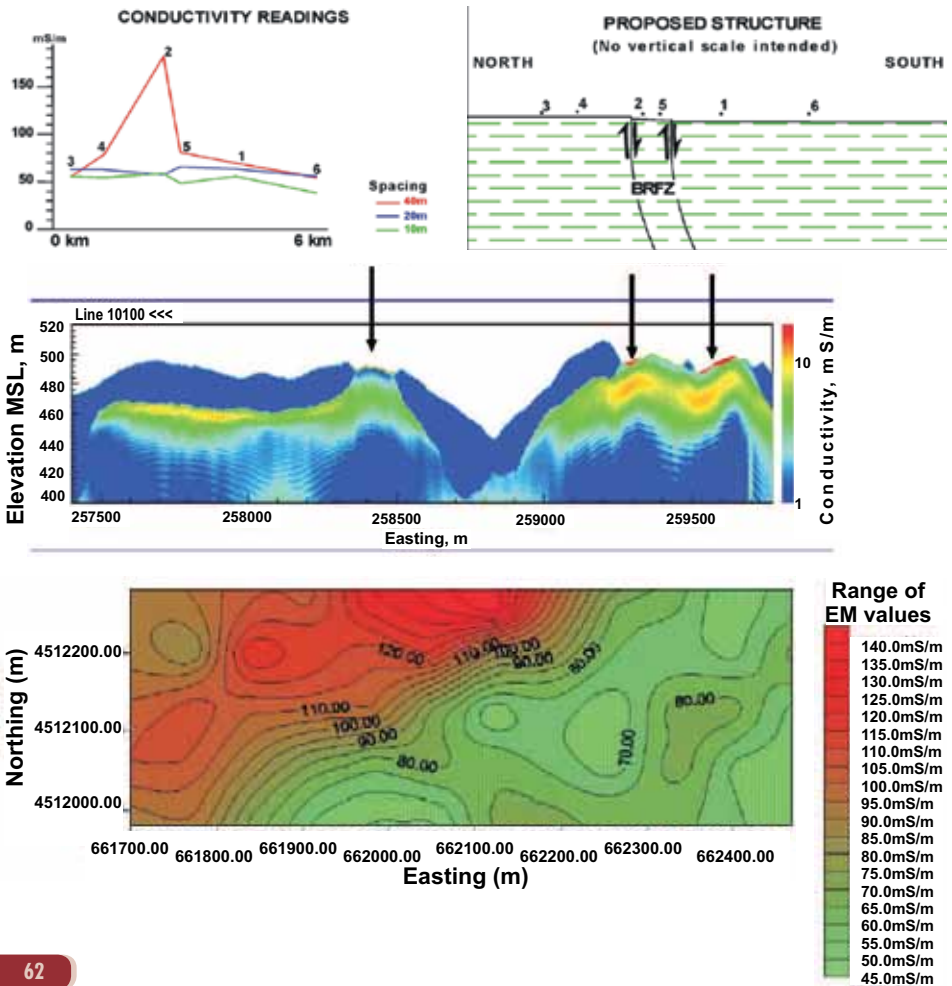
▶ Time-domain or transient electromagnetics (TDEM or TEM)

The transient electromagnetic (TEM) method is usually associated with the exploration for deep conductive ore deposits and is well suited to mapping targets in the depth range 10–1 000 m[49]. The method is, however, also applicable to geothermal exploration, general geological and bedrock mapping, groundwater exploration, groundwater contamination studies, engineering investigations and buried metal detection[50, 51]. As will be seen in later chapters, TEM also definitely has a role to play in addressing certain coal mining and exploration problems.

Fundamental principles

In TEM surveys one typically uses the combination of a relatively large ungrounded transmitter (Tx) loop and a smaller receiver (Rx) coil. The Tx loop may be as small as approximately 10 m x 10 m, or may measure a few hundred metres a side. The Rx coil is no more than approximately 1 m in diameter. The TEM method is based on the 'off-time' impulse response approach: an alternating transmitter current is set up in the Tx loop. This alternating current is abruptly terminated and, in accordance with Faraday's law, the rapid reduction of current, and of the associated primary magnetic field, induces an electromotive force (emf) in the nearby subsurface[49, 50.] The induced secondary currents are initially concentrated directly below the transmitter loop, but diffuse down and outward with time (**Figure 3.24**).

Figure 3.24 The TEM method
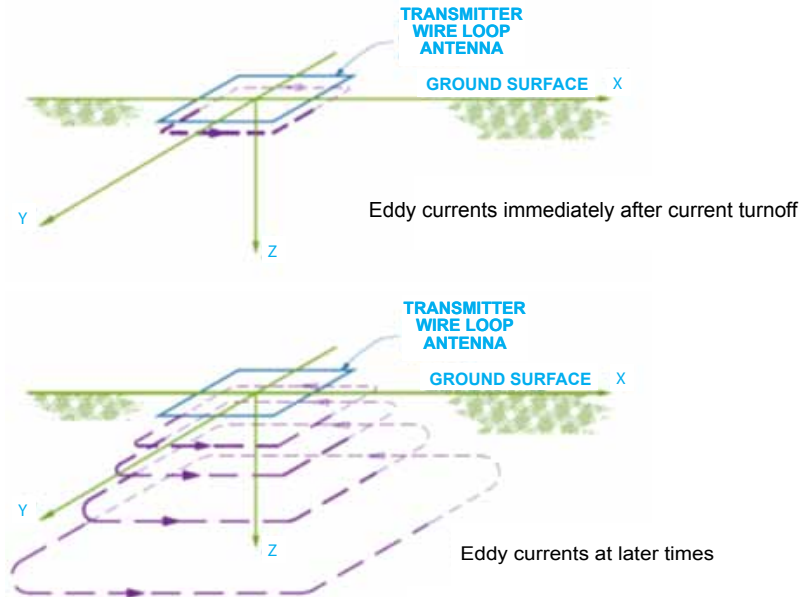
Following current termination the transmitted signal can be represented as current filaments propagating outwards and downwards with time[49, 51] .

The magnitude and rate of decay of the induced currents are functions of the conductivity, size and shape of the conductors. The TEM receiver measures the secondary magnetic field induced by these currents in the subsurface over a predefined period. Analysis of the transient decay is carried out by sampling the amplitude at numerous time intervals (and over many transmitter cycles, to enhance the signal-to-noise ratio).

By analysing the resulting decay curves one can derive information about the conductivity structure of the subsurface. For example, conductors with moderate resistivity will be associated with a rapidly decaying magnetic field; in good conductors with low resistivity the decay will be slow; in very resistive material, little or no current and secondary magnetic field will be induced.

A great advantage of TEM is that once the target has been energised we are no longer interested in the transmitter response. Measurements are made only of the response of the target. An associated limitation, however, is the quick exponential decay of the secondary field, which limits the effective depth of investigation. For this reason, TEM prospecting relies on systems with a large dynamic range, that can measure relatively large as well as extremely small signals. Furthermore, in cases where greater depths of investigation are pursued, the transmitter area and/or current is usually increased in an effort to enhance the signal-to-noise ratio.

Survey strategies

Traditionally, TEM surveys have been done with the large Tx loop and smaller Rx loop described above. Nowadays smaller cart-mounted TEM systems such as NanoTEM[51] or even boat-towed systems are available, but for the purpose of this discussion we will focus on the traditional large-loop systems. The Geonics TEM47 system is a commonly used TEM instrument of this type. Such a system is typically employed in one of three surface configurations (**Figure 3.25**):
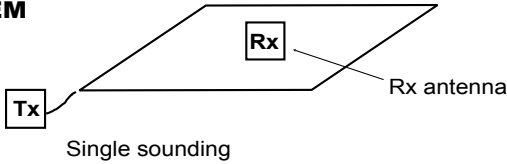
a) Fixed-loop soundings
b) Moving-loop profiling
c) Fixed-loop profiling

It is also possible to utilise a downhole profiling configuration in which a receiver probe is used along the length of a borehole. Downhole TEM is typically used to probe for conductive ore bodies that occur at depth and in close proximity to exploration boreholes.
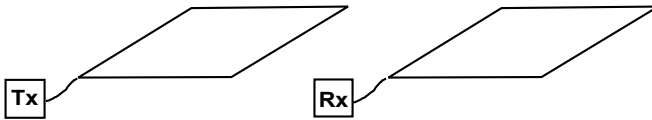
In TDEM one must trade off depth of exploration against target definition in terms of conductivity, extent and orientation. The greatest exploration depth is obtained with large fixed-loop systems; however, the associated large half-space responses and current gathering make target detection difficult. Better spatial resolution, albeit at a shallower depth, is obtained with a moving transmitter configuration and a short inter-coil spacing. These variations in survey requirements make system flexibility an important design consideration.

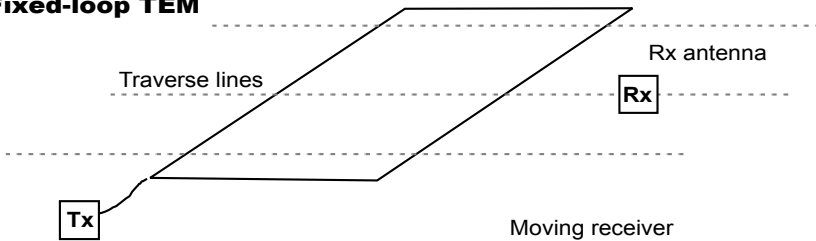**Figure 3.25** Typical TEM survey configurations; after Zonge, 2009[51]

In-loop TEM

Rx

Tx

Rx antenna

Single sounding

Moving-loop TEM

Tx

Rx

Fixed-loop TEM

Rx antenna

Traverse lines

Rx

Tx

Moving receiver

The purpose of the TEM survey and the anticipated geoelectrical scenario will determine the optimal survey configuration and survey parameters. One might be interested in obtaining cross-sectional images of conductivity along selected profiles. In this case, the moving-loop approach may be most applicable. If obtaining depth slices of conductivity over an area is the prime objective, then a large fixed-loop approach may be the best option. The different profiling approaches can also be combined to extract the maximum spatial conductivity information from a TEM survey.

Link between measured and Earth parameters

As was mentioned earlier, the decaying currents in the subsurface conductors will be indicative of the type of conductors present in the subsurface: good conductors are associated with slow decay, while poor conductors (highly resistive geological material) will have little or no decay. These differences in decay rate will manifest in the measured rate of change of the associated decaying secondary magnetic field. Examples of different decay curves for different subsurface conductivities are shown in **Figure 3.26**. Here the decay curves are

normalised measured voltages versus time plots. **Figure 3.27** shows the typical process of converting measured parameters to Earth parameters. The decay curve is converted to an apparent resistivity plot. The apparent resistivity is simply a derived parameter that makes the graphical analysis of decay curves easier. A one-dimensional (layered Earth) interpretation of such apparent resistivity curves can then be done through a combination of forward modelling and inversion: a layered Earth model is assumed/estimated that might have produced the measured curve. The response of the model is then compared and the model updated until the model response closely matches the observed response. This iterative process can be automated through so-called inversion algorithms.

Figure 3.26 Examples of TEM decay curves[51]
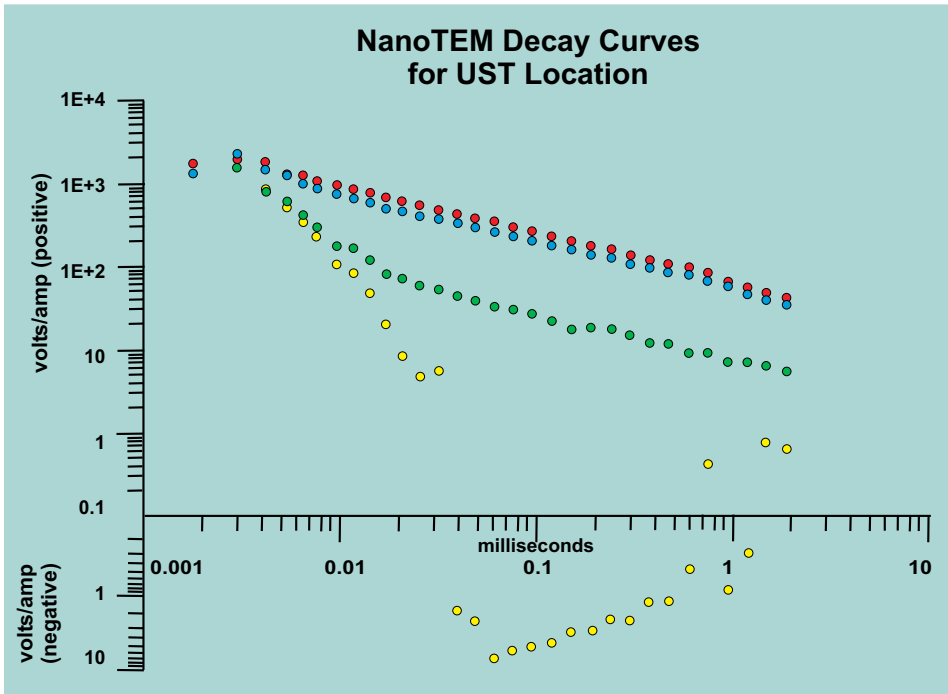
Conductive targets are characterised by slow decays (red and blue), moderately conductive ground (green) yields a faster decay, while over resistive ground the decay will be very rapid (yellow).

Figure 3.27 Example of normalised voltage decay curve, apparent resistivity sounding curve and derived one-dimensional geoelectric section[49]
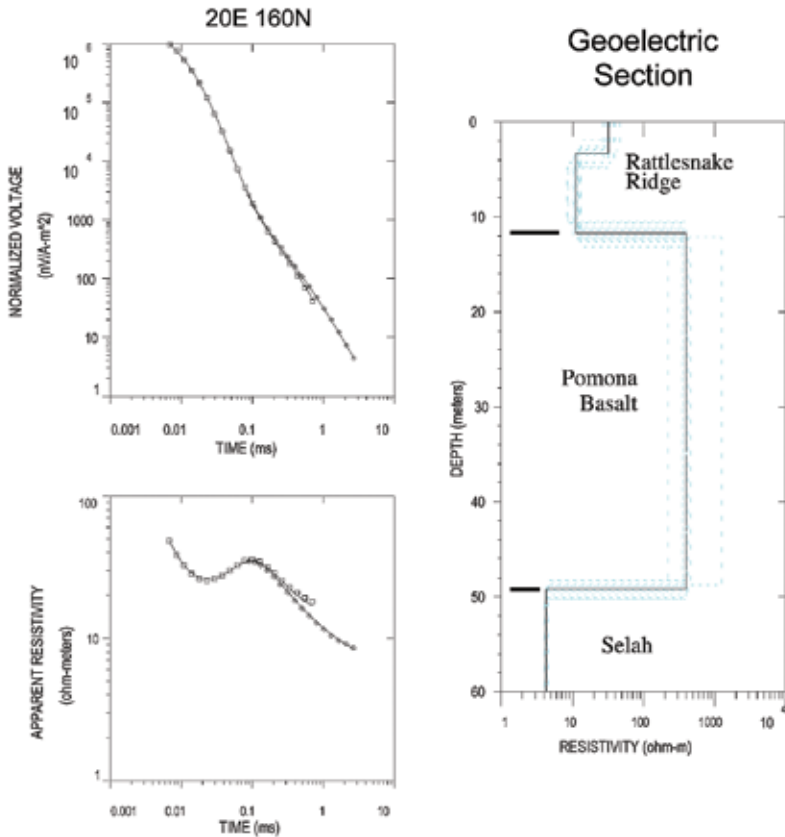
The discussion above applies to one-dimensional depth soundings over layered Earth scenarios. Obviously, in cases where the subsurface structure cannot be approximated by a layered Earth, or where resistivity information over a large area is required, a conductivity profiling approach would be more appropriate and one would have to use two-dimensional or even three-dimensional processing and interpretation approaches.

Survey output examples

It was mentioned earlier that the output from TEM surveys can be individual TEM soundings, a sequence of in-line soundings (profile) or a grid of soundings (or several closely spaced TEM profiles). Some one-dimensional sounding curves and derived layered Earth models were shown in Figures 3.26 and 3.27. In cases where the subsurface deviates from a layered Earth, the sounding curves will indicate the presence of localised/isolated resistivity

anomalies, which may, in fact, be the desired target. To obtain additional information on lateral resistivity variations relating to such targets, the output of several sounding stations or TEM profiles can be combined to produce two-dimensional TEM profiles or resistivity-depth sections or horizontal time (depth) slices (**Figures 3.28** and **3.29**).

Figure 3.28 Example of two-dimensional TEM section[51]

Smooth-model TEM resistivity
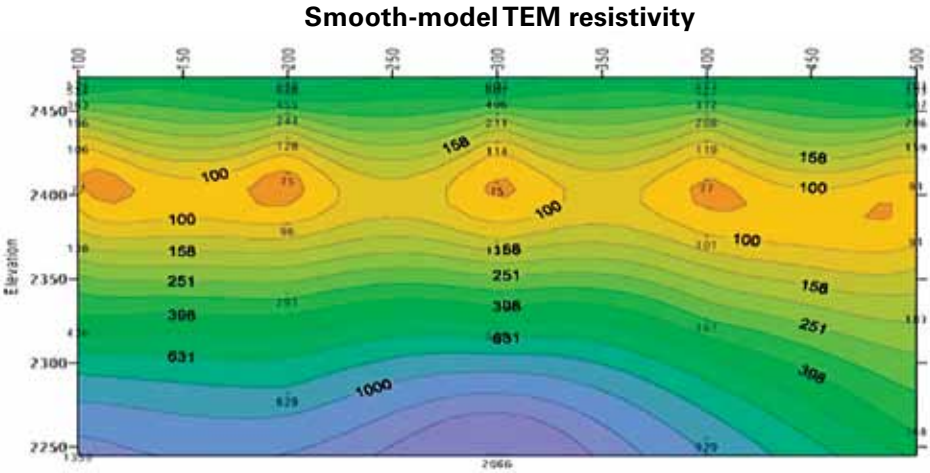
Figure 3.29 Example of two-dimensional TEM horizontal time slice[51]
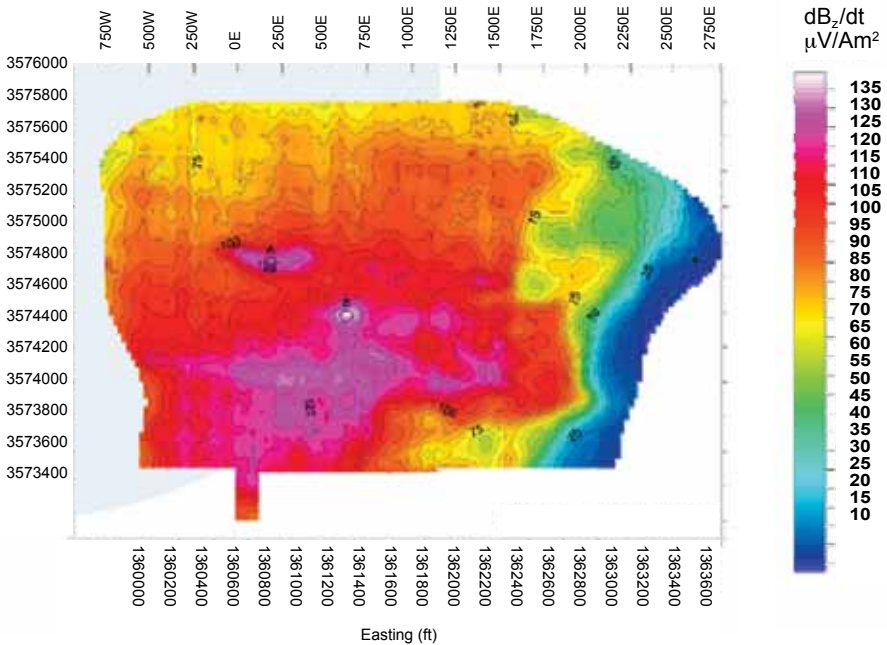
▶ Controlled source audiomagnetotelluric (CSAMT) method

The magnetotelluric (MT) method is based on the relationships between magnetic micro-pulsations, telluric currents and conductivity structures. These relationships were explained independently and almost simultaneously by Professors L. Cagniard[52] in France (1953) and A. Tikhonov[53] in the USSR (1950). Traditionally, the MT method was used to deduce the deep structure of the Earth (> 1 km) through the measurement of both orthogonal magnetic (H) and electric (E) fields at surface over a wide but low frequency range (0.001–100 Hz) to derive soundings of apparent resistivity versus frequency, which can be interpreted as true resistivity versus depth sections.

The source field for MT measurements is provided by magnetotelluric pulses. These are generated naturally at low frequencies in the ionosphere or magnetosphere (Figures 3.30a and b). As MT measurements were needed at higher frequencies, it became desirable to augment natural source fields with applied fields – above 1 kHz and particularly around the 2 kHz region, where the natural field signals are weak or absent. Goldstein and Strangway (1975) summarised the theory for a grounded electric dipole on a layered Earth and presented field and model results to extend their method, now called the controlled source AMT or CSAMT method[54]. In summary: measured changes in E and H over time, over a frequency range of approximately 100 kHz to .0001 Hz or lower, are used to derive the electrical resistivity structure of the subsurface. Figures 3.31 and 3.32 schematically show the typical artificial CSAMT source setups and the five field components that are measured in MT prospecting.

(a)

(b)

Figure 3.30a and **b** Natural sources of low frequency MT fields are due to interaction between solar winds and the Earth's magnetic field and lightning. *(Photos sourced from http://commons.wikimedia.org and authored by NASA and Rainer Knäpper, respectively.)*
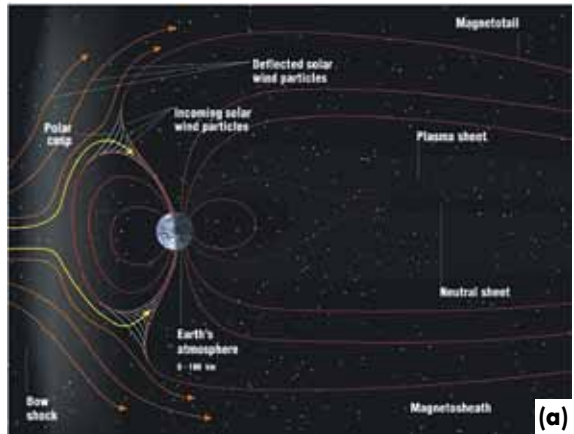
Figure 3.31 For near-surface MT exploration, higher-frequency artificial sources are required
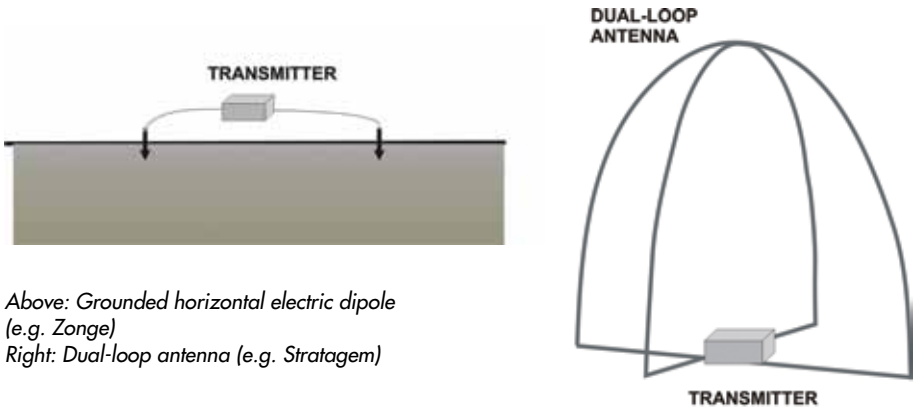
Above: Grounded horizontal electric dipole
(e.g. Zonge)
Right: Dual-loop antenna (e.g. Stratagem)

Figure 3.32 The five measured components in MT surface measurements of the Earth's natural electrical (E) and magnetic (H) fields when using an orthogonal dipole (E_{xy}) and coil (H_{xyz}) setup
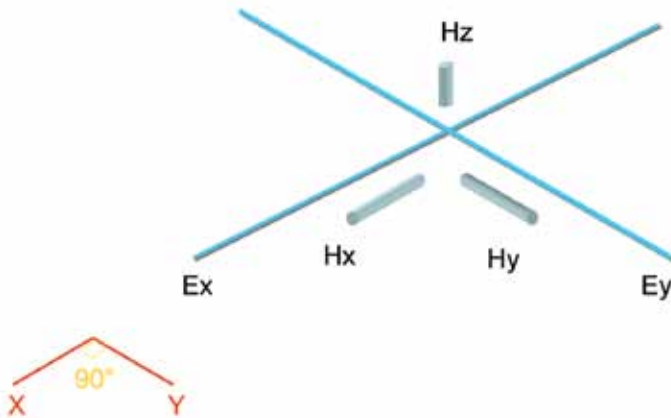
Fundamental principles

Figure 3.33 summarises the theory underlying the CSAMT method. It is assumed that a horizontal current sheet is set up above the surface of the Earth. This current induces a uniform primary magnetic field H_0. Controlled spectral fluctuations of H_0 induce a varying primary electric field E_0 that causes currents to flow in conductive Earth materials. These currents in turn induce a secondary electromagnetic field. The electrical impedance can then be defined as the ratio of the electric to magnetic fields:
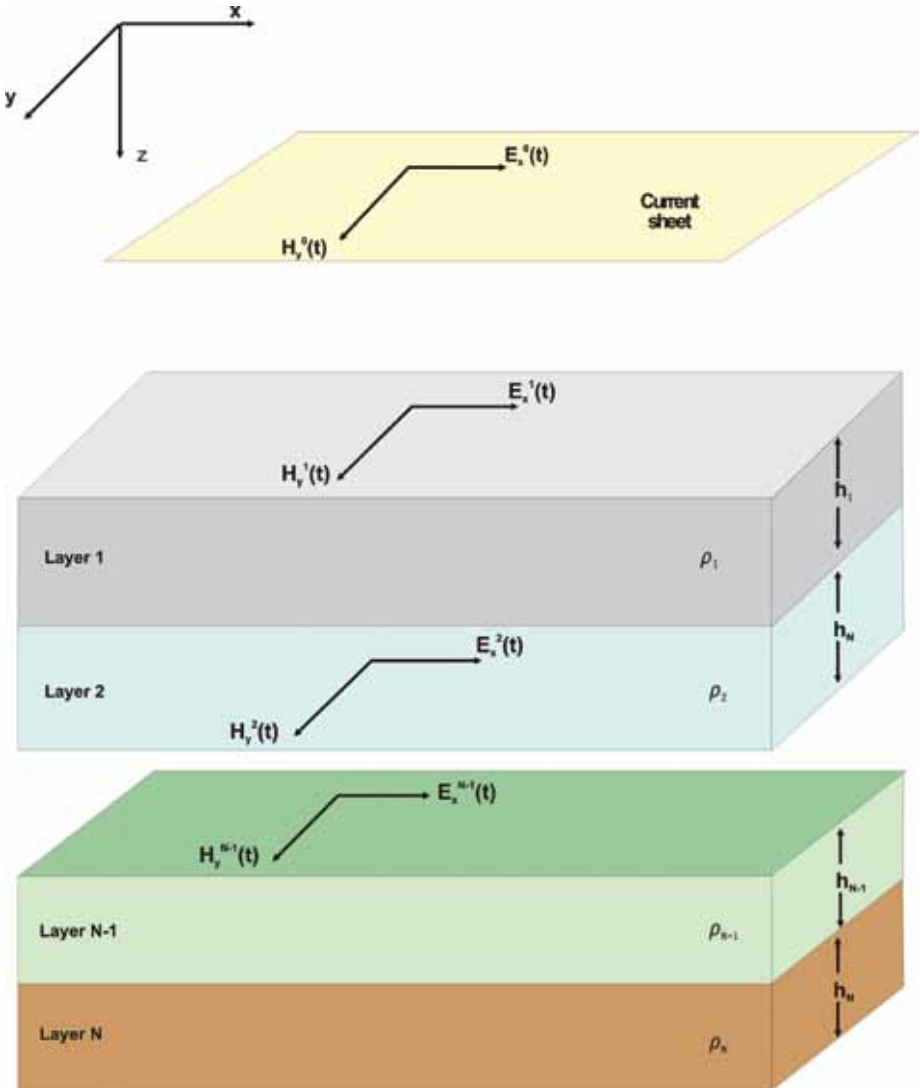
$$Z_{xy}(\omega) = \frac{E_x(\omega)}{H_y(\omega)} = \frac{\omega\mu}{k} \qquad (3\text{-}13)$$

Apparent resistivity is defined as the scaled magnitude-squared impedance:

$$\rho_{a,xy}(\omega) = \frac{1}{\omega \mu_0} \left| \frac{E_x(\omega)}{H_y(\omega)} \right|^2$$

(3-14)

The relevant electric and magnetic field components for the various layers in a layered Earth are used to derive the apparent resistivity (**Figure 3.33**).

**Figure 3.33** Schematic relating to MT impedance and apparent resistivity derivation

Survey strategies

For the purpose of this publication, the typical **Stratagem** configuration (see **Figure 3.34**) will be considered since it is the most likely system to be employed in near-surface exploration. This illustrates the field configurations for conducting sounding on a 20 m x 20 m grid pattern.

**Figure 3.34** Typical 'Stratagem' CSAMT sounding array
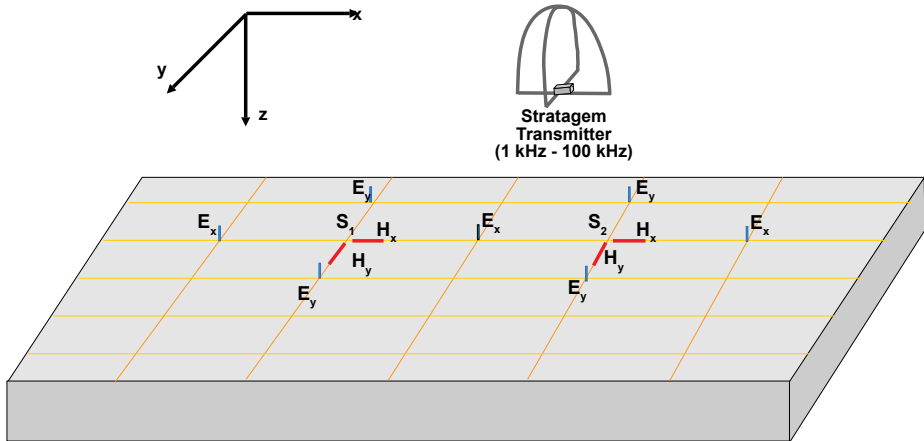
S_1 and S_2 represent two successive sounding centres;
E_x – Electric dipole along traverse and perpendicular to geological strike;
H_y – Magnetic coil parallel to geological strike;
E_x and H_y form spectral pair for Transverse Magnetic (TM) mode of survey;
The E_y, H_x pair is referred to as the TE or Transverse Electric mode.

Link between measured and Earth parameters

CSAMT data processing is a fairly involved and specialised task. **Figure 3.35a** shows the typical raw data field records: the various electric and magnetic field components are recorded as functions of time and then Fourier transformed to the frequency domain. Sounding curves (**Figure 3.35b**) can then be derived for the transverse magnetic and transverse electric modes, as well as true resistivity depth sections. A sequence of collinear soundings can be combined to generate resistivity cross-sectional (two-dimensional) images such as the one shown in **Figure 3.36**.

Figures 3.35a and **b** CSAMT raw data and derived sounding curves

(a)

(b)
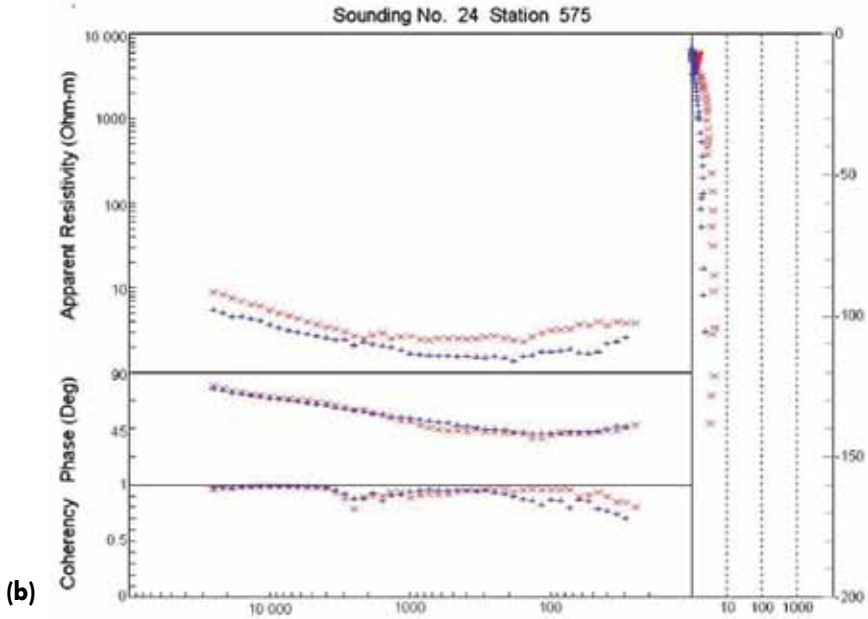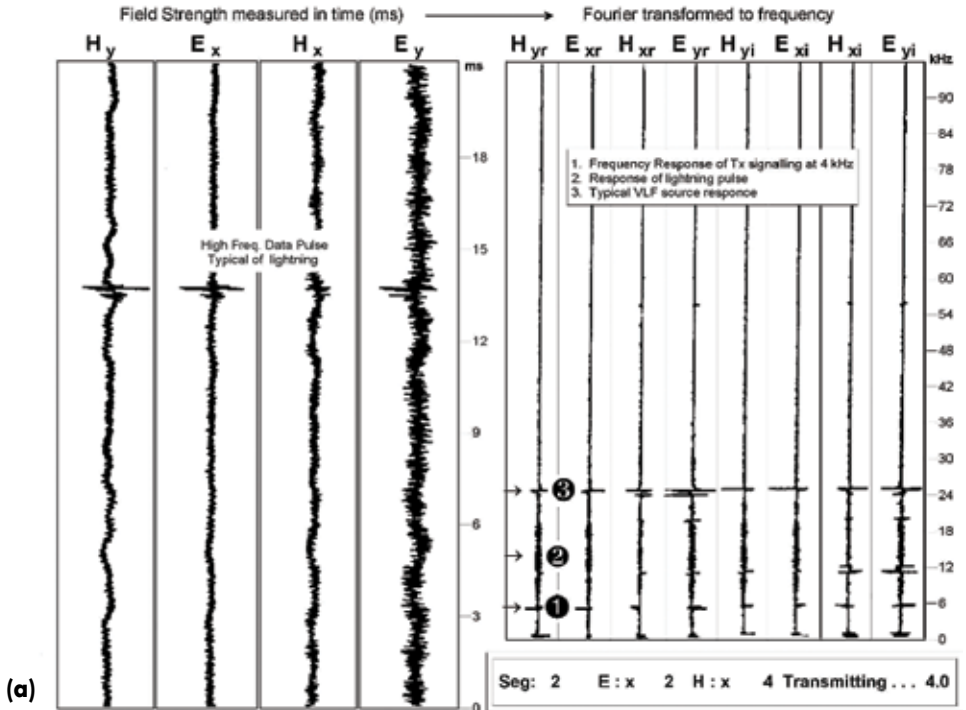
Figure 3.36 Example of CSAMT two-dimensional cross-sectional resistivity image, horizontal (depth) slice and geological interpretation based on resistivity sections
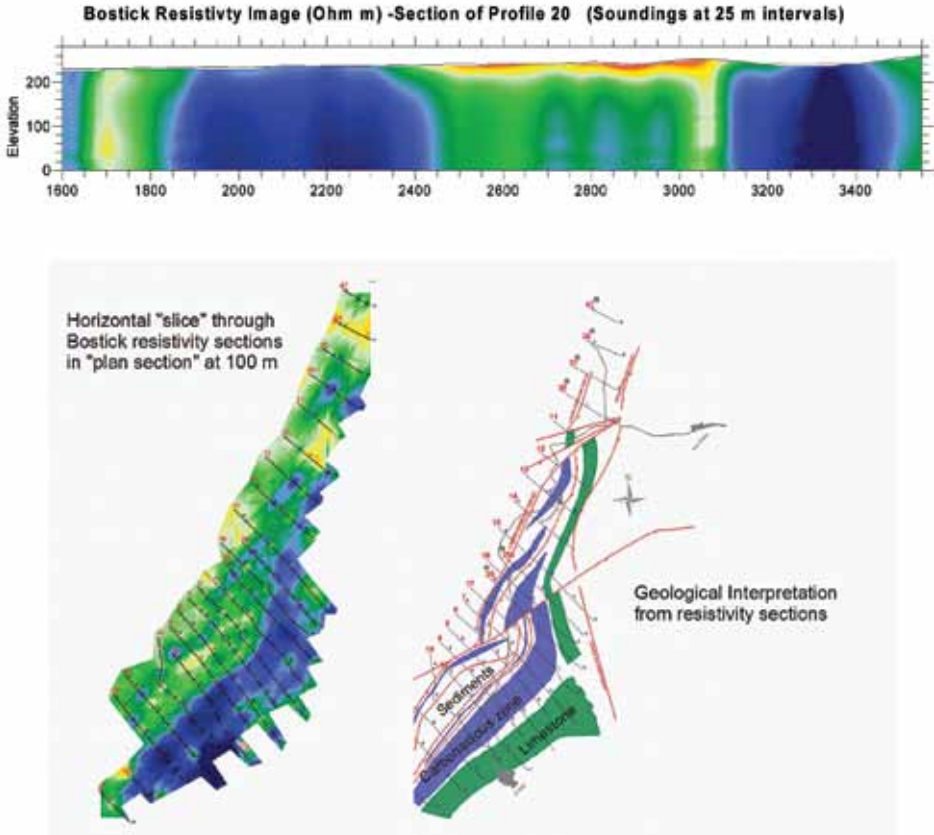
Advantages and disadvantages of CSAMT

CSAMT is an attractive option for near-surface exploration. The equipment is lightweight and portable and consequently good production rates and access to difficult sites are possible. The interpretation procedures for CSAMT have been well developed and fast turnaround times are possible (provided the appropriate interpretation software and skills are readily available).

Arguably the most attractive feature of CSAMT is that it provides better resolution than gravity and magnetics at far greater depths (from surface to a few hundred metres). However, the resolution of CSAMT is not as good as that of seismics and probably no better than TEM or electrical imaging. Furthermore, the CSAMT inversion (image reconstruction) methods rely on smooth models, which make interpretations in structurally complex areas fairly challenging.

▶ Seismic refraction

Seismic refraction was traditionally a key geophysical method used in oil exploration, but these days it is used more and more for terrain investigations and civil engineering projects; for example, foundation and dam construction. Seismic refraction is a wavefront method and assumes a layered Earth model. The underlying physical principle for the refraction method is Snell's Law in optics, extended to seismic waves[28].

The limitations of the seismic refraction method are related to its inability to define individual thin geological horizons when they become deeply buried and if their reflection coefficient is similar to the neighbouring layers. Referring back to **Table 2.1**, the physical properties that dictate whether targets can be detected by the seismic methods are density and seismic wave velocity; these parameters control the reflection coefficient of layer boundaries. The seismic refraction method is also limited where steeply dipping geologic layers occur or where geological layering is not well defined, for example in karst environments.

In terms of resolution, the seismic refraction method can be placed somewhere between the gravimetric method (low resolution) and the seismic reflection method (high resolution).

Fundamental principles

During a seismic survey the subsurface is energised using a sound (shock) source. This source induces strain in the subsurface. The source (hammer, explosives, guns or vibrators) induces different types of strains in the subsurface: tension due to pressure, tension due to pulling and tension due to shear strain. Seismic waves act just like normal sound waves or the waves you see when you throw a stone into water (the stone hitting the water acts as a point source and the waves are generated in a circular fashion around it). Any radial line through these waves describes a wave train of amplitude versus time. Similarly, the circular seismic wavefronts propagate down into the subsurface, and the wavefront becomes flatter as its radius of curvature increases. For all practical purposes, the wavefront striking the geological interfaces may be considered flat.

P-waves and S-waves

There are two types of seismic body waves (**Figure 3.37**): P-waves or primary waves are the faster type. P-waves are also known as compressional waves, as they are responsible for pushing and pulling in the direction of wave propagation. The secondary, or S-waves, are slower than P-waves, and they move particles perpendicularly to the direction of wave propagation. S-waves are also known as shear waves. Applied seismic methods rely almost exclusively on P-waves.

Note that there are also surface waves such as Rayleigh and Love waves associated with seismic shocks/explosions, but for the purpose of this discussion we will not elaborate further on these.

Figure 3.37 P-wave and S-wave motion
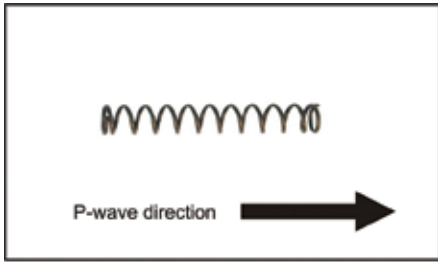
In P-wave motion the particles expand and compress much like the motion of a compressional spring
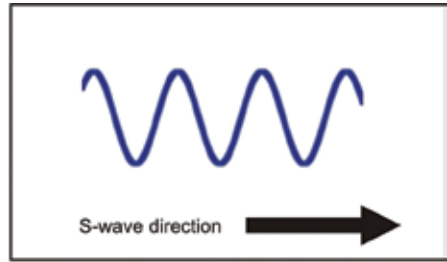
In S-wave motion the particles move up and down, perpendicular to the wave direction

When the wavefront hits a layer boundary we can apply Snell's Law (**Figure 3.38a**) to understand the concept of seismic refraction. The incident wave will be reflected off the boundary (provided there is a sufficient property contrast between the two layers) and at some angle of incidence a portion of the energy is refracted along the boundary interface (**Figure 3.38b**). This angle is called the critical angle or angle of refraction. Due to the stress that the refracted wave exerts on the interface, each point along the interface acts as a secondary source and sends out rays towards the surface, which can be detected by geophones.

Figure 3.38a and **b** Snell's Law applied to seismic waves

θ_i Angle of incidence
θ_r Angle of reflection
θ_a Angle of refraction
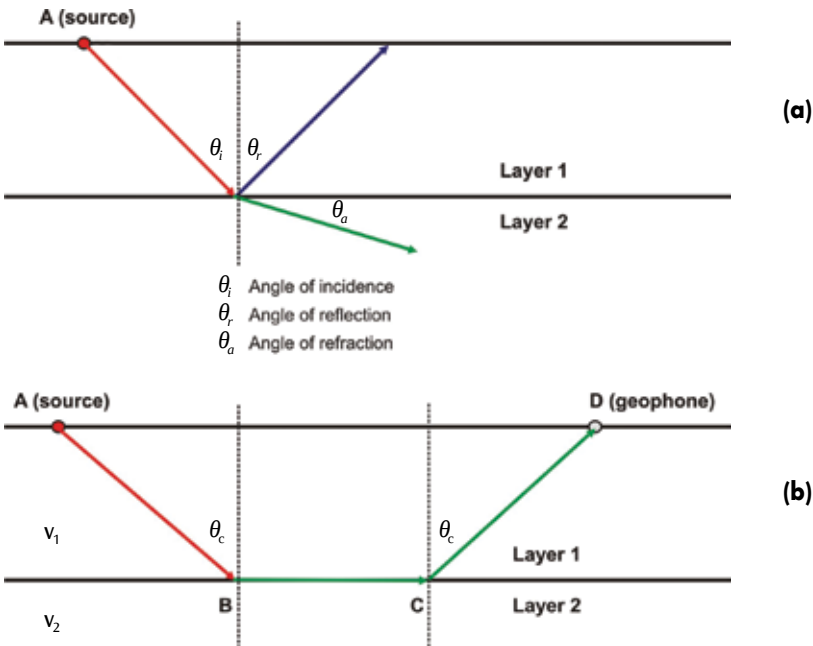
If the geophone D is close to the source A, then the first response detected will be the direct wave between A and D. If D is located a bit further away, the refracted wave will arrive before the direct wave because $v_2 > v_1$. The higher velocity is associated with the higher density of the deeper layer. It is the refracted part of the wave that provides us with the required information about the subsurface.

Survey strategies

A typical refraction setup is shown in **Figure 3.39**.

**Figure 3.39** Typical seismic refraction setup
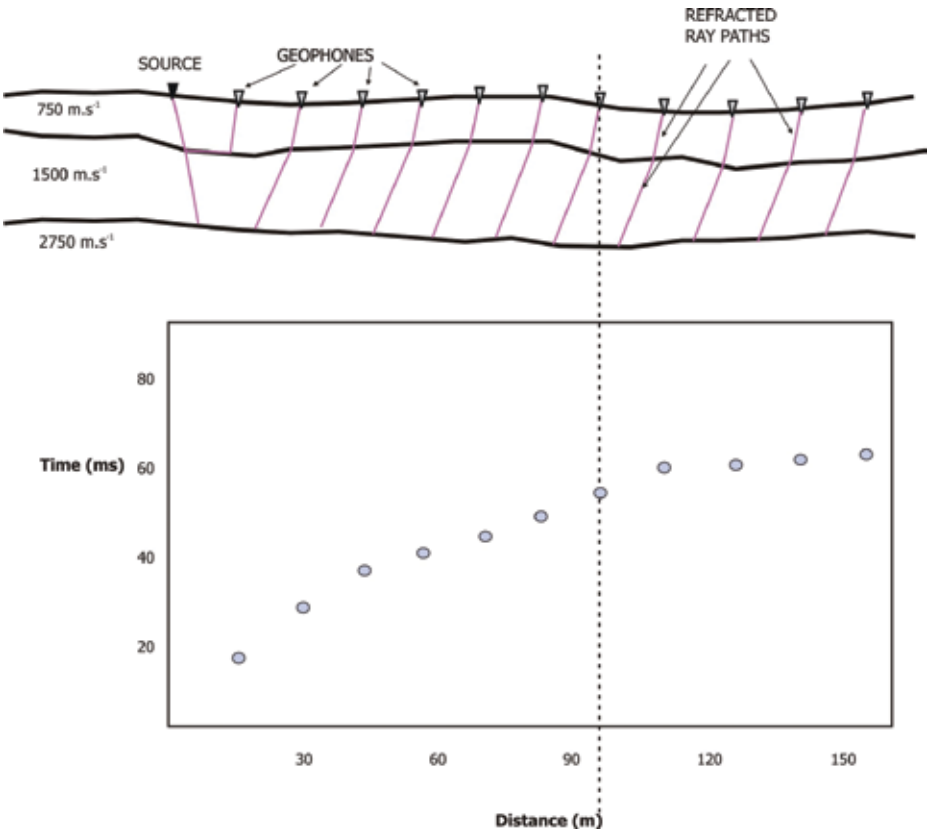
The seismic refraction survey is performed by putting out geophones on a survey line. These geophones are equal distances apart. The source is typically used at five different positions on each spread:

- ■ **Left offshot**   (source located some distance to left of first/leftmost geophone)
- ■ **Left end-on shot**   (source coincides with first/leftmost geophone)

- **Split-spread shot**   (source located in middle of geophone spread)
- **Right end-on shot**   (source coincides with last/rightmost geophone)
- **Right offshot**   (source located some distance to right of last/rightmost geophone)

   During a seismic refraction survey, we record the amplitude of the seismic waves at the geophones as a function of time. The first arrivals are picked for all the traces in the survey spread, resulting in a travel time curve. These travel time curves can have different shapes, depending on the properties and geometry (thickness and dip) of the subsurface layers. From these plots it is possible to determine the seismic velocities of the layers, and how many layers are present. Each slope on the two-way travel time plot indicates a different layer, and the slope of the layer is inversely proportional to its velocity; m=1/V. **Figure 3.40** shows an example of a refraction two-way travel-time curve and associated survey and model geometry.

Figure 3.40 Seismic refraction two-way travel time curve example
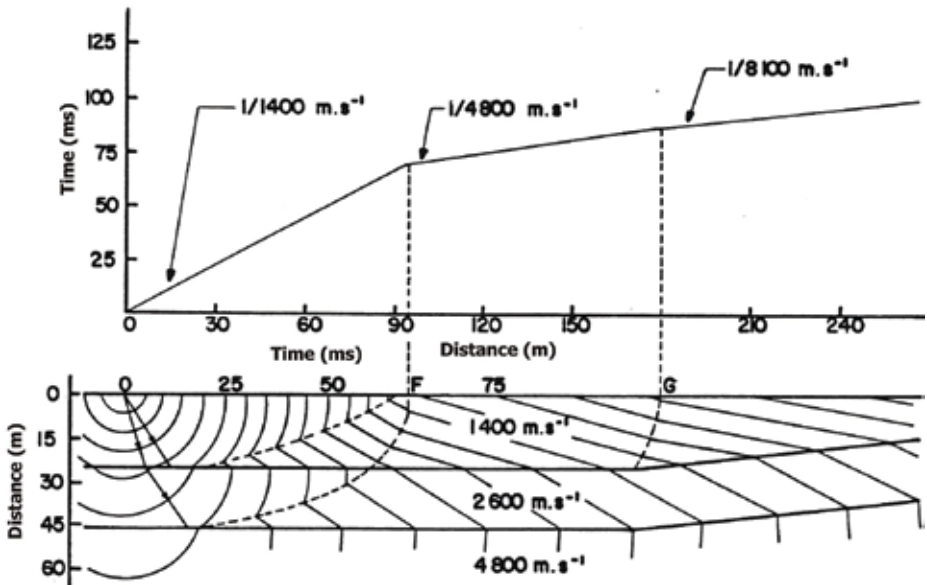
Link between measured and Earth parameters

Seismic waves are elastic waves with velocity

$$v = f\lambda \tag{3-15}$$

where f is the frequency and λ is the wavelength. The waves that are important in seismic refraction are the longitudinal P-waves or pressure waves. Seismic waves that travel through the subsurface are attenuated due to absorption and friction. The energy of the seismic wave

through the subsurface is directly proportional to the square of its amplitude. If the seismic wave moves away from its source position, its energy is dispersed over a larger surface; that is, the energy per unit area decreases as the distance from the source position increases. The amplitude (I) of a wave at distance r is given by:

$$I = I_0 \frac{r_0}{r} e^{-\alpha r} \tag{3-16}$$

where I is the amplitude at distance r, I_0 is the amplitude at distance r_0 and α is the absorption coefficient.

According to Huygens' Principle, every point on the wavefront is a source for a new wavefront. With distance, the radii of these wavefronts increase to such an extent that they form an almost flat wave surface. When these waves reach a geologic interface, they behave according to Snell's Law (refer to **Figure 3.37**):

$$\frac{\sin \theta_i}{\sin \theta_r} = \frac{v_i}{v_r} \tag{3-17}$$

where i denotes the incident wave and r denotes the reflected wave.
If $\theta_r = 90^0$ (incident wave moves along the boundary, becoming the refracted wave) then the critical angle is defined by

$$\sin \theta_{crit} = \frac{v_i}{v_r} \tag{3-18}$$

For interpreting travel-time curves, we will only discuss one of the popular graphical methods used, namely the Plus-Minus method[55]. This is an approximate method by which the depth of a plane seismic refractor may be determined beneath each receiver (geophone), using forward and reverse travel times. The forward and reverse travel times are plotted against offset, from which the seismic velocity of the weathering layer and the refractor(s) can be determined.

The so-called 'Plus' values are obtained by adding the forward and reverse travel times at each receiver, and subtracting the total travel time from the sum. The plus values, in effect, are the intercept times determined by constructing a tangent to the time-distance curve at each receiver station. 'Minus' values are calculated by subtracting the forward travel time from the reverse travel time at each receiver station. A plot of Minus values versus offset provides information on the refractor velocity and the number of layers present. A spreadsheet tool was developed by Fourie and Odgers to interpret seismic refraction data[56]. The spreadsheet calculates velocities for each layer:

$$M = \frac{1}{v_i} \tag{3-19}$$

The left and right velocities of the refractor are used to calculate the geometric average of the velocity:

$$v_1 = 2\frac{v_L v_R}{v_L + v_R} \tag{3-20}$$

The k-factor is then

$$k = \frac{v_0}{2\sqrt{1 - \left(\dfrac{v_0}{v_1}\right)^2}} \tag{3-21}$$

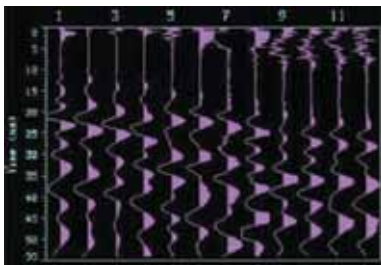The 'Plus' time values at each receiver are obtained by:

$$T_{plus} = T_{forward} + T_{reverse} - T_{total} \tag{3-22}$$

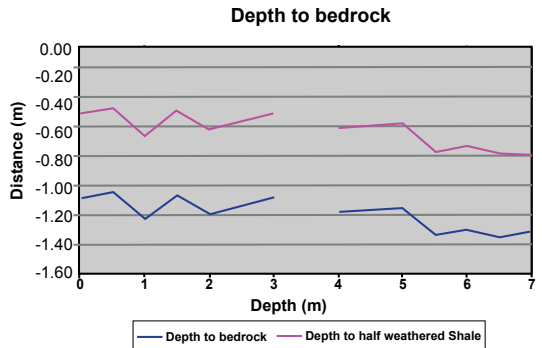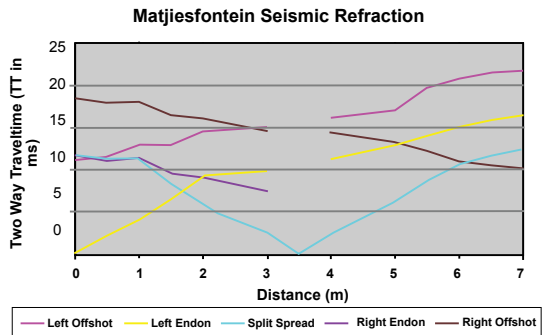Finally, the depth to the refractor is obtained by:

$$D = kT_{plus} \tag{3-23}$$

Survey output example

Figure 3.41 Example of typical seismic refraction survey results[57]

Top left is a screenshot of the recorded seismic traces; top right shows the time-distance plots for the various source locations; bottom image shows the calculated depth of the layer boundaries

▶ Seismic reflection

Seismic reflection is a high-resolution exploration method that differs in several aspects from seismic refraction, as covered in the previous section. In this introduction, the important differences between reflection and refraction will be highlighted. The rest of the section discusses some of the aspects relating to data acquisition and processing. It is arguably these aspects that set the seismic reflection method apart from seismic refraction and other geophysical techniques. Seismic (reflection) data acquisition is a fairly involved and highly specialised exercise, and the same can be said of the subsequent data processing and interpretation. For these reasons, it is also significantly more expensive to apply than other ground-based methods.

Fundamental principles

In a reflection seismic survey, a signal is transmitted from a source, which is generally on the surface. The signal is reflected off the boundaries between geological horizons and is recorded by a receiver as a seismic trace (record of signal amplitude versus time). As the signal travels through the subsurface, it is modified in shape and strength, and the character of these changes may be used to infer properties of the subsurface. Depths to reflecting surfaces may also be determined if the seismic velocities of the geological horizons are known. The resolving capability of seismic reflection is determined by the input frequency, the velocities of the geological horizons and the frequency filtering of the subsurface.

So, in what ways do the reflection and refraction approaches differ? Consider again a seismic source, located on the Earth's surface, which generates elastic seismic waves that propagate into the Earth. The speed at which the waves travel is determined by the seismic impedance of the host material. Seismic impedance is defined as the product of the seismic wave velocity and the density:

$$Z = v\rho \tag{3-24}$$

When the seismic wave encounters a sudden change in acoustic impedance, for example, at layer boundaries, some of the energy will reflect off the interface, while some will refract through the interface (refer back to the schematic of **Figure 3.38**). The reflection method is concerned primarily with detecting and analysing the reflected seismic energy, while the refraction method focuses on the special case of critically refracted energy. Each geophone in a seismic configuration records the amplitude of the seismic signal as a function of time and these recordings are displayed as wiggle traces. A seismogram comprises a series of wiggle traces for a given spread of geophones.

The schematics in **Figure 3.42** illustrate how these two methods are applied in practice, while **Figure 3.43** shows how refracted and reflected seismic signals manifest differently on seismic outputs.

Figure 3.42 Schematics showing the different geometries typically employed in seismic refraction (top) versus seismic reflection surveys[58]
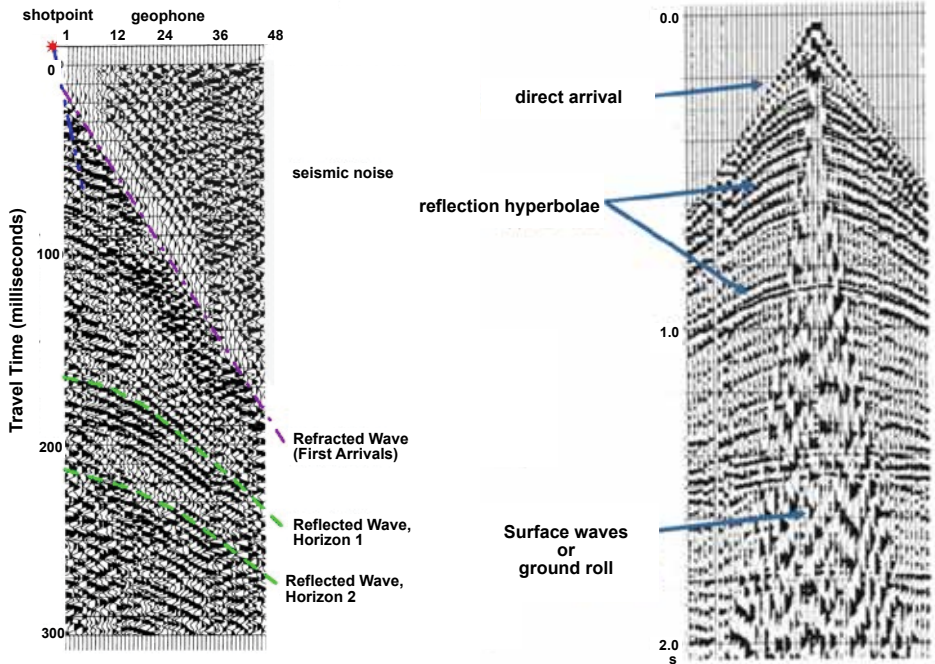
Seismic Refraction Geometry
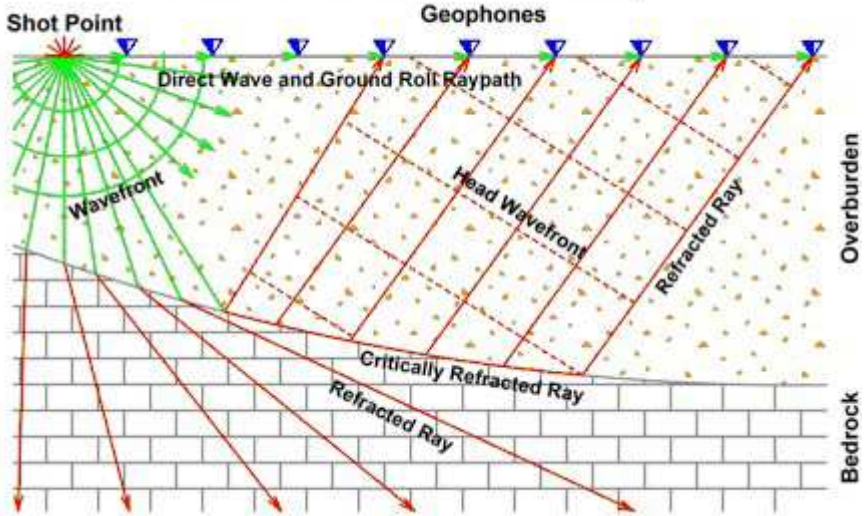
Seismic Reflection Geometry
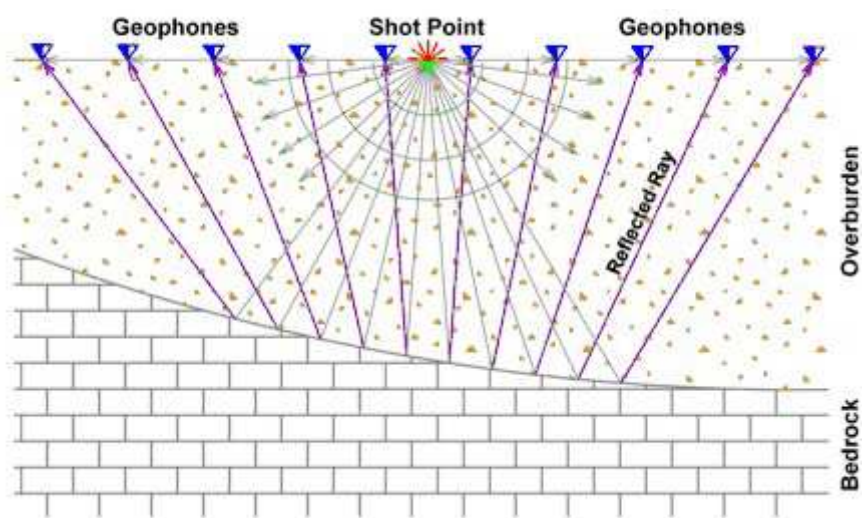
Figure 3.43 Example seismograms revealing how the refracted and reflected signals manifest differently, depending on the survey geometry[58, 59]


Survey strategies

Data acquisition

As with seismic refraction, reflection seismic surveys can be conducted using different source-receiver geometries. The two most commonly used geometries are end-on (common-shot) and split-spread shots (**Figure 3.44**). The type of environment of the survey area and the objective of the survey dictate the mode of survey. Note that the two example seismic records shown in **Figure 3.43** are for end-on and split-spread geometries, respectively.

Seismic survey environments are varied, ranging from well consolidated ground to marshes, desert sands, ice and snow. Surveys can also be done across water bodies using towed arrays. Large arrays of sources and receivers can be deployed to increase the input and recording signal strength and up to 1 024 channels may be used. Sources range from continuous (e.g., Vibroseis) to impulsive (hammer, airgun or explosives).

Figure 3.44 End-on shot (top) and split-spread shot (bottom)

End-on shot (common shot) gather

Split-spread shot
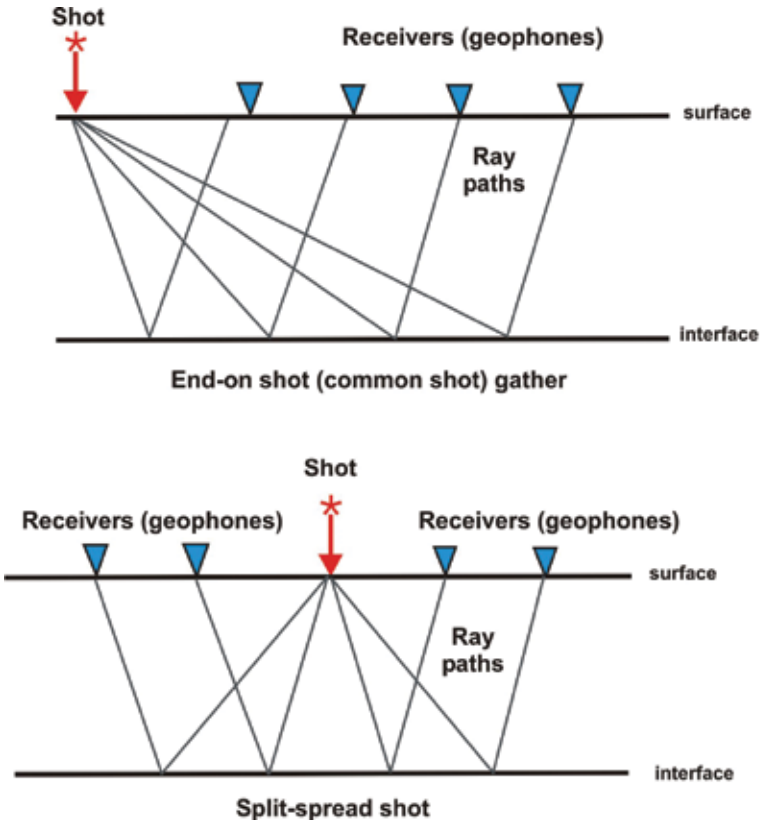
Calculation of fold coverage

During a seismic reflection survey a large number of shots is used. This means that certain traces (travel paths) from different shots will be reflected from the same spatial position. The number of traces that will reflect from the same spatial position is called the '*Fold*'. The fold is calculated with the following equation:

$$Fold = \frac{(number\ of\ geophones)\,\Delta G}{2\,\Delta S} \tag{3-25}$$

where ΔG is the geophone spacing and ΔS is the shot spacing.

A larger fold will improve the signal-to-noise ratio due to the fact that more traces reflect from the same spatial position. It is thus important to obtain the largest possible fold, which is achieved by increasing the number of geophones and decreasing the shot spacing. As one might expect, higher fold surveys are more time-consuming and costly.

Vibroseis source

We will now describe the Vibroseis source type, as it is widely used in seismic reflection. It consists of a large truck and a base plate that is pressed against the surface by the weight of the truck (**Figure 3.45**). The truck is fitted with a vibrator that can change its vibrating frequency. Usually the frequency is varied from low to high over a period, and this is called the 'sweep'. Depending on the depth of investigation, one to five Vibroseis trucks can be deployed. The duration of the sweep depends on the survey objectives. A longer sweep is generally used for a larger depth of investigation.

Figure 3.45 Vibroseis source

Although the details are beyond the scope of this discussion it can be noted that the data is recorded in an incoherent format that requires a number of mathematical processes to convert to a sequential trace format. These processes include cross-correlation and demultiplexing.

Seismic data processing

Seismic data processing is a fairly involved process, but can be broken down into three stages, namely pre-processing, pre-stack processing and post-stack processing. Below is a listing of the typical steps with a brief description of each step.

Pre-processing

Pre-processing comprises the steps needed to prepare the data for processing. These include vibroseis cross correlation, demultiplexing and gain recovery.

Pre-stack processing

During pre-stack processing the following concepts are addressed:

- **Survey geometry –** The physical location and elevation of each shot and receiver are entered into the trace headers of the recorded data. The shot and receiver co-ordinates are used to determine the bin locations for sorting into common midpoint (CMP) gathers. The elevations are used to calculate the refraction static correction.
- **Signal amplitude decay –** Reflected signals from deep interfaces may have very low amplitudes on the gain-recovered traces (from pre-processing). It is thus necessary to scale the signal for interpretation. The true amplitude of the reflection events is lost through

these gain adjustments; however, if one is only interested in the location of the reflectors, the true amplitude information is not important. Gain-recovered traces show a considerable decrease in amplitude with time, and a spherical gain correction can be applied to correct the amplitudes of the data. Data also loses amplitude through friction of the subsurface and this loss is a function of time, scattering and distance. This can be countered by applying a gain function such as automatic gain control (AGC). AGC methods use a sliding scaling window (time-variant trace equalisation) to achieve the desired output level.

- **Noisy trace editing** – Noisy and bad traces will degrade the results obtained by the final stack. These traces are identified and 'flagged'. Flagged traces are excluded from further processing.
- **First break (refraction) picking** – The identification of the arrival times of the refracted waves is called first break picking. It enables the statistical calculation of the static corrections (thickness of the weathering layer) to be applied to the data.
- **Muting** – Air waves and ground roll often obscure the information of the shallow near-offset traces due to their low velocities. This can be countered by applying a top end surgical mute. Muting is achieved by removing all amplitudes within a specified region (mute zone) and replacing them with zeros.
- **Refraction static corrections** – Static corrections are designed to remove the path-dependent variations in shot-to-receiver travel times due to the low velocity layer (LVL) or weathered zone. Due to the low velocity of this layer, small variations in the layer may cause significant static (time) shifts in the data. **Figure 3.46** shows the situation that needs to be addressed. Static corrections can be made either by first conducting a seismic refraction survey to characterise the LVL, or by picking the refraction information from the reflection data and then applying a static correction through the processing software. The correction aims to move the start time of all the seismic traces to a common datum.

Figure 3.46 Static correction problem illustrated
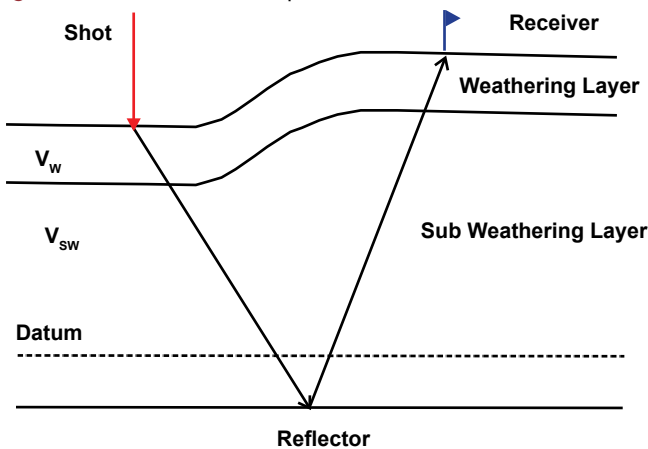
- **Normal moveout correction (NMO)** – The normal moveout correction (NMO) is necessary in seismic reflection surveys due to the fact that a horizontal reflector appears on a common mid-point (CMP) gather as a hyperbola. This is due to the fact that travel times increase when larger shot-receiver offsets are used. All traces that reflect from the same CMP need to be stacked to form one stacked trace. If these reflections are not in the same time position, the result will be a 'smeared stack' with a very poor signal-to-noise ratio.
- **Velocity analysis** – The main purpose of a velocity analysis is to obtain the best velocity for the NMO correction. This will result in the optimum stack of the seismic reflection data. Sometimes in literature it is also referred to as the 'stacking velocity'. Two methods exist of determining the stacking velocity of seismic CMP data: velocity spectrum analysis and constant velocity stack (CVS). For further details on these processes the reader is referred to one of the many publications discussing these processing steps.
- **Deconvolution** – The primary objective of deconvolution is to improve the temporal resolution of the seismic data and thereby improve the accuracy of the interpretation. Deconvolution can be described as convolving with an inverse filter, with the purpose of retrieving the reflectivity function of the seismic trace. During deconvolution we attempt to remove the input signal from the recorded seismic trace to obtain the reflectivity function of each geological boundary.

    Deconvolution can be applied during pre-stack processing or during post-stack processing. Pre-stack deconvolution is primarily used to remove effects of finite input signals for the seismic data, such as explosive sources and vibroseis sweeps. Post-stack deconvolution is primarily used to remove interbed multiples and spiking, and predictive deconvolution is also used for this purpose.

- **Stack** – The stack produces the final result for the seismic survey. Areas of interest are identified on the stack and the characteristics of these features are used to determine the parameters for post-stack processing to improve the stack. **Figure 3.47** shows an example of a stacked seismic section.

Figure 3.47 Example of a stacked seismic section

- **Residual statics** – Lateral velocity variations and near-surface inhomogeneities cause the moveout of an event in a CMP gather to deviate from the idealised hyperbolic shape. The result is distortions in the NMO-corrected CMP gathers and a less than perfect stack.

    An improvement in stacking quality is achieved by the calculation of residual static corrections before a NMO correction is performed on the CMP gather, by making the moveout hyperbolic. Velocity analysis must be repeated to improve the stack.

Post-stack processing

The purpose of post-stack processing is to improve the quality of the stacked seismic section and improve the accuracy of the interpretation. Processing of the stacked section is much faster due to the significantly smaller size of the data. Typically post-stack processing includes migration, filtering and gain.

Migration

Migration locates events on a seismic section in their true spatial positions by collapsing the hyperbolic diffraction patterns towards the diffractor (typically a fault) and by correcting for the distortion in position and amplitude of dipping reflectors observed on non-migrated sections. The latter distortion occurs because observed reflection events are plotted directly below the geophone locations, rather than their true spatial position. **Figure 3.48** schematically illustrates this concept.

**Figure 3.48** Schematic of the migration principle
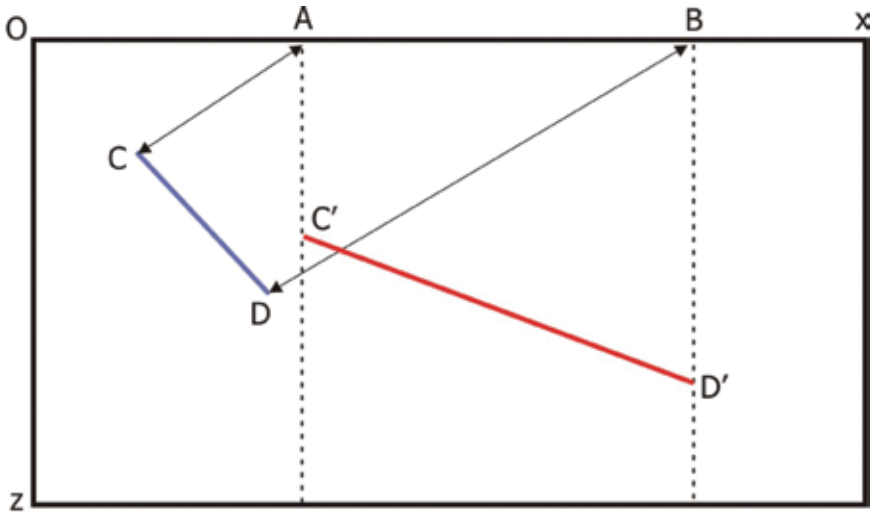
The dipping target CD manifests at the apparent location C'D' in the non-migrated time section. Migration will cause the reflection to move updip, and to be steepened, shortened, and mapped onto its true subsurface location.

Processing sequence

The processing sequence of seismic reflection data is summarised in the flow chart in **Figure 3.49**.

Figure 3.49 Standard Reflection Seismic Data processing sequence
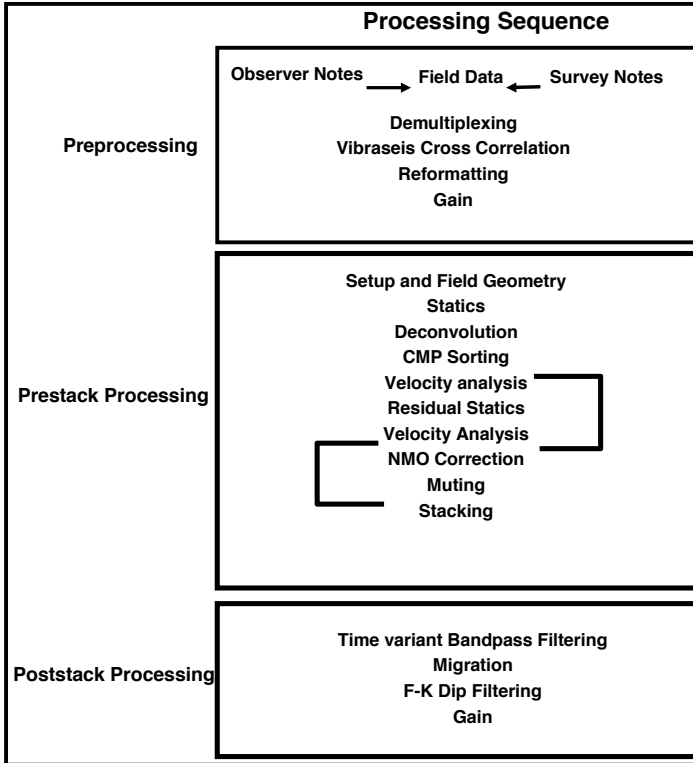
Seismic reflection survey examples

Seismic reflection can play a role in mapping variations in coal seams, especially for deeper coal deposits where other geophysical methods (including refraction) would not be able to achieve the required range and resolution. **Figure 3.50** shows some examples of the application of seismic reflection to coal seam mapping.

Figure 3.50 Examples of how seismic reflection can be used to map the continuity of coal seams and structures that compromise seam continuity[60, 61]
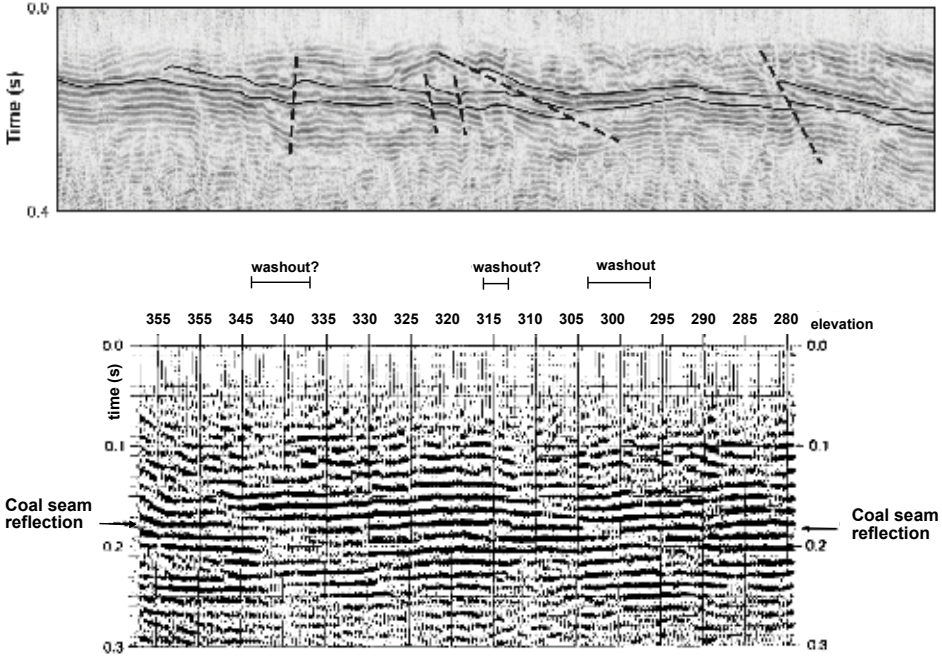
▶ Multichannel analysis of surface waves (MASW)

The traditional seismic methods discussed in the preceding sections exploit body waves. In those sections, only a brief reference was made to the other type of seismic waves, namely surface waves. In the multichannel analysis of surface waves (MASW) method we make use of these surface waves (in particular Rayleigh waves) to extract information about the subsurface. MASW is typically used for the following applications:

- Mapping of soil stiffness
- Shear wave measurements
- Measurement of depth to bedrock
- Detection of fractures and low velocity zones
- Detection of voids

MASW can be used as an alternative method in areas of high interference from man-made sources (buildings, tar roads, pavements, etc.) which prevent one from using the electrical resistivity or seismic refraction methods. It is also an attractive and relatively easy method for producing shear wave profiles without the requirement for boreholes, as used in cross-hole and down-hole seismic surveys.

Fundamental principles

MASW utilises the dispersive nature of surface waves to map the variation of shear wave velocity with depth. Long wavelengths travel deeper into the subsurface than shorter wavelengths and sample different velocity regions of the subsurface. By generating a range of short to long wavelengths the dependence of shear wave velocity on depth can be determined. The variation is represented as a dispersion curve which is then inverted to produce a shear wave velocity profile.

MASW can be used in active or passive mode, as determined by the field setup and the source characteristics. The active method uses an artificial source, such as a dropped sledgehammer or weight, at a certain offset distance from a linear array of receivers. The passive method can use background noise, originating from man-made sources or natural ones, such as waves or even earthquakes. In this case the array may be linear, cross-shaped, circular, etc. The advantage of the passive array is potentially better penetration, as background sources typically have lower frequency surface waves than active sources. The active method allows one to measure continuous shear wave velocity sections by systematically moving the linear array (receivers and source) laterally, allowing the measurement of lateral changes in velocity. A combination of the passive and active methods may be used, depending on the objectives of the investigation and the site conditions. The presence of surface waves can be easily identified on a seismic record as shown in **Figure 3.51**.

Figure 3.51 Surface waves identified on a 24 channel seismic record. The body waves (P-wave) are visible in the time band below 100 milliseconds
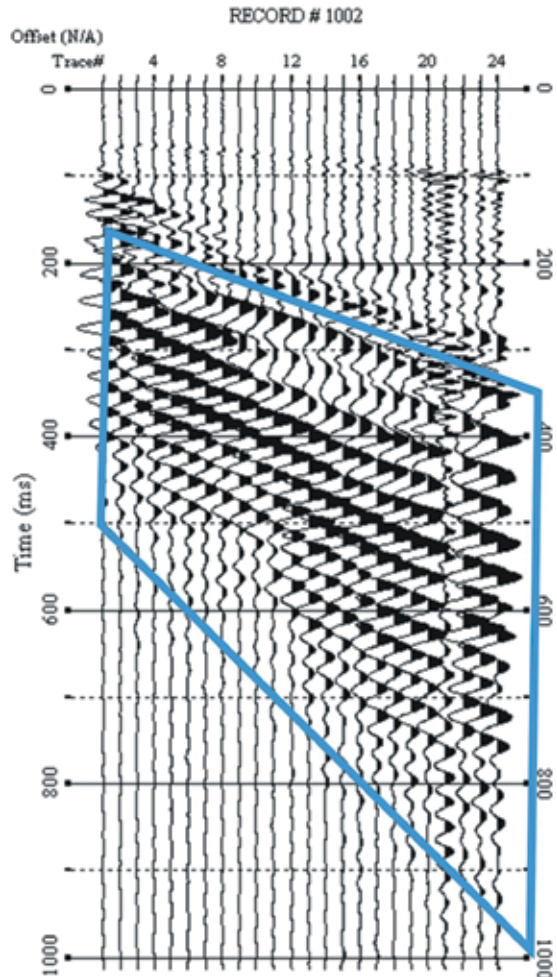
Survey strategies

The MASW method uses an array of geophones (typically 12 to 24) with a single shot location offset from the line. Each shot location then produces a single one-dimensional shear wave velocity profile. The entire geophone array as well as the shot location are then moved along the line. A two-dimensional section is generated by combining all the one-dimensional profiles. As a rule of thumb, the spread length should be similar to the depth of investigation; typically, a 1–2 m geophone spacing is used for penetration up to 30 m. Low-frequency geophones are preferred, as the depth of penetration depends on the ability to generate and record low frequencies (4.5 Hz natural frequency geophones are recommended). A sledgehammer is an effective source for penetration of 20–30 m. The passive method makes use of square or circular arrays to provide better imaging of low frequency events. A land streamer system can be used for rapid deployment of the geophones on tarred and smooth areas, as spike coupling is then not required for effectiveness (**Figure 3.52**).
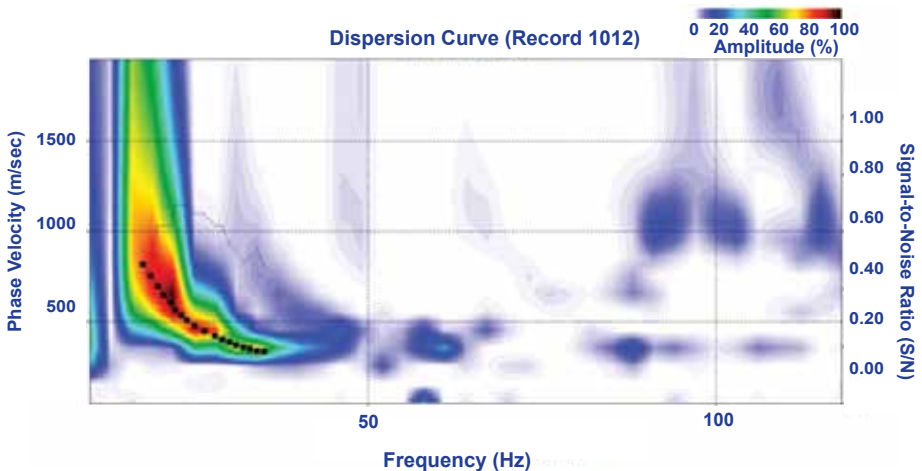
Figure 3.52 Land streamer system in operation

## Link between measured and Earth parameters

Overtone analysis is used to generate a dispersion curve for a particular shot location as shown in **Figure 3.53** below:

Figure 3.53 Example of MASW overtone analysis

Plotting of the phase velocities as a function of frequency allows for the identification of the fundamental mode of the surface wave and the extraction of the surface wave as indicated. The dispersion curve is then inverted for every shot location to produce a one-dimensional shear wave velocity profile, as indicated in **Figure 3.54**. The individual one-dimensional profiles are then combined to produce a section, as shown in **Figure 3.55**.

Figure 3.54 Shear wave profile (blue). The dotted points are the dispersion measurements, and the solid line is the forward model from the shear wave profile.
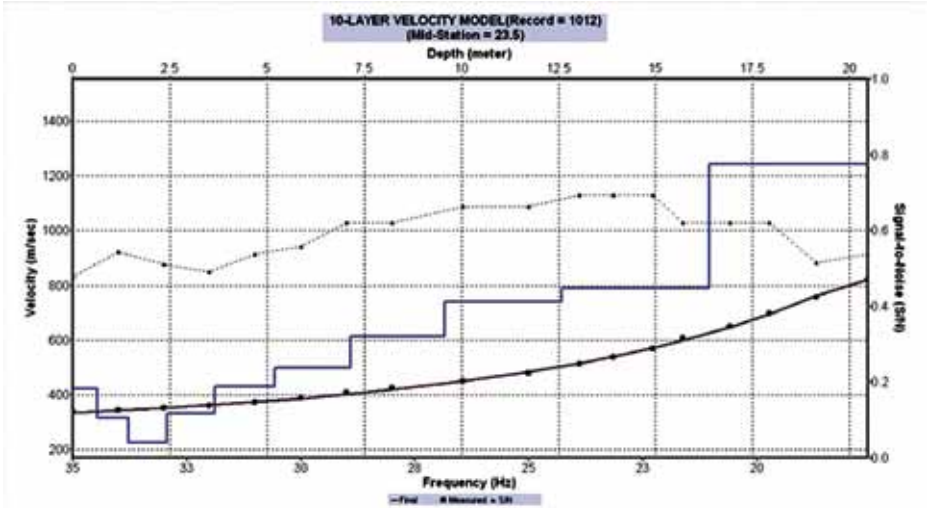
Figure 3.55 Continuous shear wave velocity section. Application was to map fractured rock which can be clearly observed as a low velocity zone in the 10–30 m chainage area.
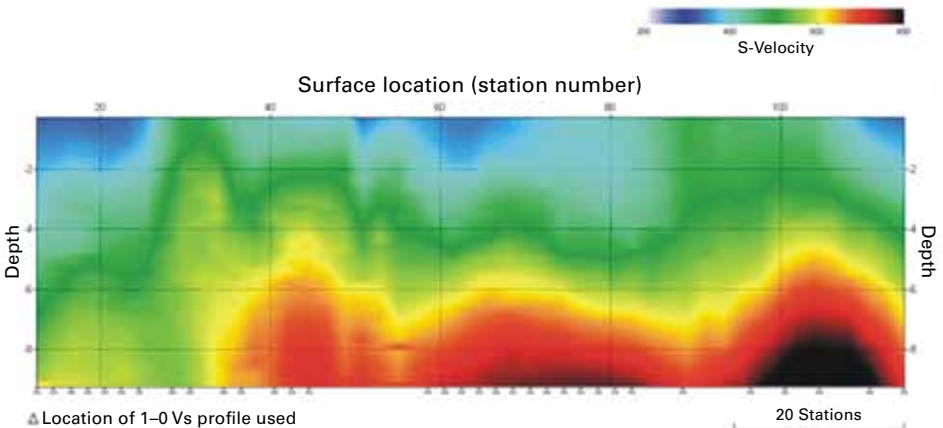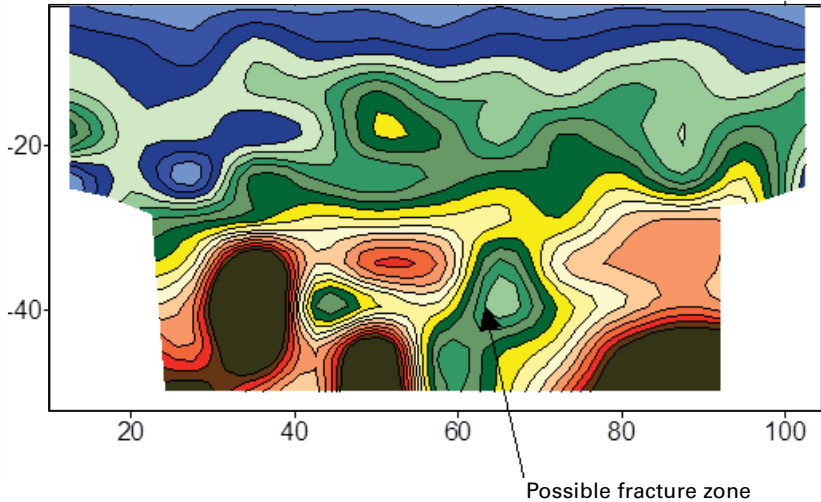
Figure 3.56 shows a further example of a typical MASW survey output. Here a two-dimensional image of Rayleigh wave phase velocity is used to detect possible subsurface fracture zones (low velocity).

Figure 3.56 Survey example – using MASW to map fracture zones

Rayleigh wave phase velocity

Possible fracture zone

▶ Wireline logging

Downhole geophysical surveys (also known as wireline logging) are very common in the petroleum industry and are routinely used for analysing rock formations. However their application in the mining industry is variable and site-specific, and also dependent on the particular environment or company. The coal industry uses downhole geophysical logging extensively for quality purposes, along with basic geophysical probes such as density and gamma measurements.

Downhole geophysical surveys vary widely in the type of data and properties that can be measured, and the information that can be derived from those measurements. These measurements are conducted for key specific applications; for example, petrophysical measurements are used for quality and grade control measurements, resource and reserve estimations etc., while structural information is used for geotechnical investigations and characterising geological structural complexities.

Downhole geophysical surveys are simple operations, and all the equipment is housed in a small truck or 4x4 vehicle (**Figure 3.57**). This includes the geophysical probes, the winch and the computer hardware and software. Borehole logging services in South Africa are provided by consulting companies such as Weatherford and Quiklog Geophysics.

Figure 3.57 Logging truck in the field

Fundamental principles

Petrophysical measurements from geophysical logs measure physical properties of rock formations based on lithological properties, which are influenced by properties like grain size, mineral composition etc. These measurements are statistical in nature, so good geostatistical measurements and sampling are required for comprehensive and reliable data. Small-diameter boreholes (< 50 mm) can be surveyed using 'slim-line tools' carrying the appropriate electronic sensors[62]. The tools are slowly winched up the hole at about 4 m per minute and nearly continuous measurements are recorded (at ~ 1 cm intervals). The digital measurements of wall-rock parameters are transmitted back to surface via conductors in the winch cable. These parameters include formation, density, resistivity, sonic velocity, magnetic susceptibility, etc., recorded as point measurements (profile data) or pixel components (images). Both cored and non-cored holes can be surveyed, and wireline logging greatly increases the information yield of the borehole for just a small fraction of the overall drilling costs. Table 3.5 below shows downhole geophysical methods, their applications and their benefits.

Table 3.5 Wireline logging parameters and tools

TOOLS	APPLICATIONS	SUMMARY OF BENEFITS
Caliper	Borehole risk assessment tool	• Detects cavings in borehole wall • Identifies large-scale breakouts, without showing orientation
Density	Petrophysical and geotechnical	• Measures in-situ bulk density of rock formations, used as a parameter for ground gravity surveys. • Used for acoustic impedance calculations, which are then useful for seismic parameter input and synthetic seismogram generation.
Neutron	Petrophysical and geotechnical	• Used for porosity measurements; however, primary and secondary porosity need to be understood and differentiated. • Because it detects presence of hydrogen, it is useful in detecting aquifers or water ingress.

TOOLS	APPLICATIONS	SUMMARY OF BENEFITS
Sonic	Petrophysical and geotechnical	• Measures compressional and shear wave velocities, which are then used to calculate elastic modulus and Poisson's ratio. • Velocity data is used for defining seismic and VSP parameters and applications, and together with density, sonic data is used for acoustic impedance calculations.
Magnetic susceptibility	Petrophysical	• Detects magnetic formations like iron ore formations, magnetic dykes, Iron-Rich Ultramafic Pegmatite bodies (IRUPs) etc. • Assists with quantitative modelling and interpretation of aeromagnetic and ground magnetic data.
Natural/Spectral gamma	Petrophysical	• Characterises natural gamma radiation, which is useful in detecting radioactive elements in rock formations. • Detects density contrasts in lithological formations. • Identifies intersections with dykes. • Used in quality control (QC) for coal and estimation of ash content in coal.
Electrical resistivity	Geotechnical and petrophysical	• Resistivity contrasts provide information on fracture aperture, secondary porosity, grain size, etc. • Detects zones of fracturing, especially where saline water flows through the fractures, hence it is useful to detect water ingress as well. • Data useful in processing and interpretation of surface and airborne geophysical surveys, particularly EM surveys.
Induced polarisation	Petrophysical	• Detects zones of mineralisation, in particular disseminated sulphides.
Fluid conductivity	Geotechnical and (to a lesser extent) petrophysical	• Differentiates fluid types by measuring their electrical conductivity. • Identifies zones of water ingress into the borehole as formation fluids have higher concentrations of minerals than borehole water.
Temperature/ Differential temperature	Geotechnical	• Measures thermal gradient around the borehole. • Identifies zones of water ingress as formation fluids are warmer than borehole fluids.
Flowmeter	Geotechnical	• Detects zones of water ingress into the borehole. • Induced flowmeter estimates flow rates at zones of water ingress.
Gyro navigation	Geotechnical	• Measures borehole deviation, without being affected by magnetic field.
Micro-resistivity dipmeter	Geotechnical	• Measures borehole tilt and azimuth. • Identification and orientation of shallow dipping strata. • Improved resolution over normal electrical resistivity.

TOOLS	APPLICATIONS	SUMMARY OF BENEFITS
Acoustic televiewer	Geotechnical	• Measures acoustic reflection and travel time. • Identifies fractures and maps their orientation using magnetometer in the tool, hence natural magnetic field effects need to be considered and filtered out. • May be used to derive stress direction. • Measures borehole tilt and azimuth. • Measures breakouts in the borehole and infers tensile fracturing. • Works only in water-filled boreholes
Optical televiewer	Geotechnical	• Similar to Acoustic Televiewer, but works in dry boreholes as well as those filled with clear water.
Checkshot surveys	Petrophysical and geotechnical.	• Maps velocity-depth profiles along the length of the borehole, which is used for seismic calculations and depth conversions. • Gives a more accurate input into synthetic seismogram models/ calculations.

Some of the more commonly used wireline tools are described in more detail below:

Density and neutron logging

Density logging is used extensively across all commodities for petrophysical and geotechnical reasons. In petrophysical measurements, density provides valid information about rock quality, and is useful for grade control, and reserve and resource estimations. Neutron logs complement density logs in that they measure porosity, which affects density measurements.

Both these tools use radioactive sources for energy, as seen below. They are kept in shields for safety reasons, to ensure that there is no leakage of radiation. **Figure 3.58** below shows a schematic diagram of a density probe in a borehole. A similar setup is observed for all other probes, the only difference being whether the probe needs to be centralised or positioned against the borehole wall.

Density logging is driven by Compton scattering and photo-electric absorption. A radioactive source will emit energy or gamma rays that bombard rock formations, scattering energy which is then captured

Figure 3.58 Schematic diagram of a density probe against a borehole wall
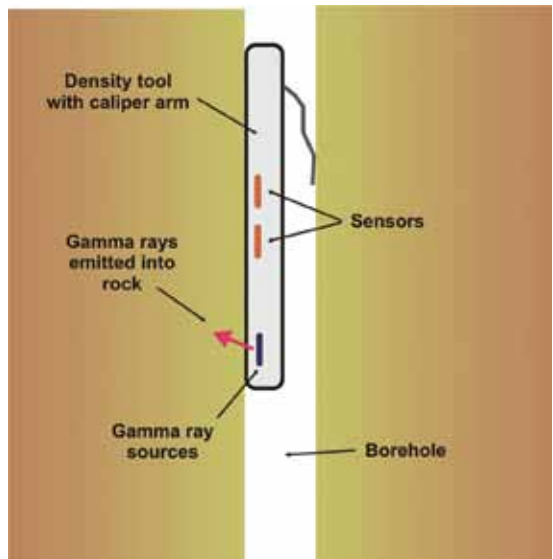
by a detector in the probe. This energy forms the basis of density measurements that are characteristic of specific lithological properties of the rock formations. The electron density is related to bulk density P through the formula:

$$\rho_e = 2\frac{Z}{A\rho}$$

(3-26)

where ρ_e is electron density, Z is the atomic number, and A is the molecular mass. Because of this relationship, calibration of density probes is of the utmost importance, especially in high-density formations like iron ore. The denser the rock, the greater the degree of Compton scattering and hence the lower the count rate of back-scattered energy to the detector. For reliable and accurate measurements all the tools need to be calibrated before and after deployment into boreholes.

Neutron logging may be used as a 'proxy' for density logging in cases where density logging is impossible or when measurements are inaccurate. This is based on the fact that neutron logging measures porosity indirectly through absorption of neutrons by hydrogen, thus giving an estimation of porosity of surrounding rock formations. Again, calibration of tools is of the utmost importance for reliable results.

Acoustic and optical televiewer logging

Acoustic and optical televiewers are the most important downhole logging tools for obtaining structural information. Acoustic televiewer logging is based on sound waves through borehole fluid and rock formations, and measures amplitude and travel time. An acoustic wave is sent through from the acoustic televiewer probe to the borehole wall while the tool is rotating through 360^0 at high speed. A high-resolution image of the borehole wall is produced, on which fractures and caving of the borehole wall can be identified. **Figure 3.59** shows how the recorded image can be 'unwrapped' and used to determine the dip and strike of an observed fracture plane.

Fractures intersecting the borehole may be open or closed, and thus care should be taken in interpreting acoustic and optical televiewer data.

Figure 3.59 Unwrapping of televiewer image and calculation of dip and strike[63]
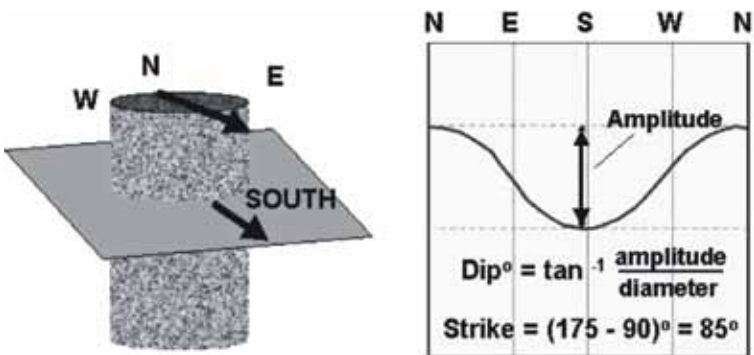
Examples of wireline logging measurements

Figure 3.60 shows a typical wireline logging result from a coal mining environment. Here the various logging tools were used to delineate the coal layer boundaries and to correlate the logging parameters with calorific value.

Figure 3.60 Example of multi-tool wireline log results from a coal mine[64]
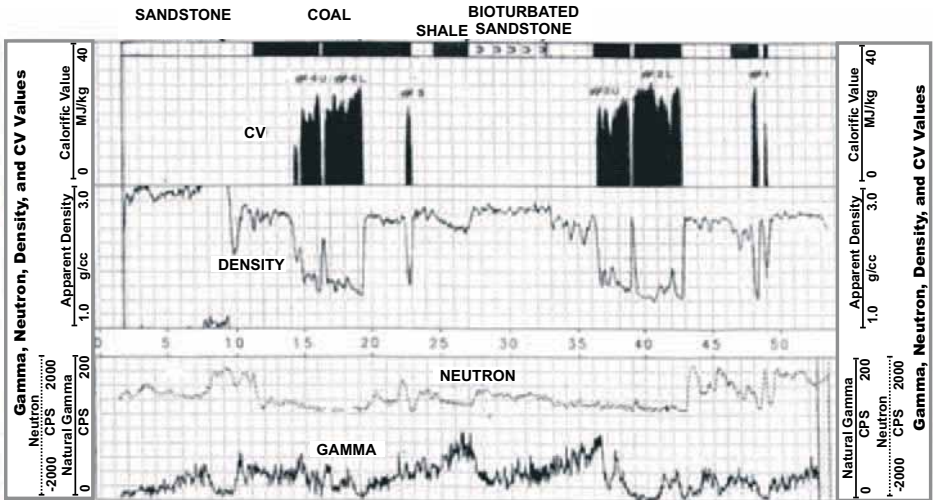
The low density signatures of the various coal seams are evident; the associated estimated calorific values are also shown.

Waterberg Coalfield (Bruce Cairncross)